STUDY OF REAR IMPACT IN LIGHT TRUCKS AND POTENTIAL INJURIES TO THE OCCUPANTS

A Thesis by

Dhruv Vikram Patel

Bachelors of Engineering, Mumbai University, 2003

Submitted to the Department of Mechanical Engineering
and the faculty of the Graduate School of
Wichita State University
in partial fulfillment of
the requirements for degree of
Masters of Science

May 2007

STUDY OF REAR IMPACT IN LIGHT TRUCKS AND POTENTIAL INJURIES TO THE OCCUPANTS

I have examined the final copy of this thesis for form and content, and recommend that it is to be accepted in partial fulfillment of the requirements for the degree of the Masters of Science, with a major in Mechanical Engineering.

_____

Dr. Hamid M.Lankarani, Committte Chair

We have read this thesis and recommend its acceptance

_____

Dr. Kurt Soschinske

_____

Dr. Bayram Yildirim

DEDICATION

To my Father Vikram, my mother Heena, my brother Minith and my Grandparents

ACKNOWLEDGEMENTS

I would like to express my sincere gratitude to my research advisor Dr. Hamid M.Lankarani for his constant help and guidance. His belief in my interest motivated me to work hard on Thesis. His constant support and guidance has helped me throughout the completion of my masters in Wichita State University.

I would also like to thank to my committee members Dr. Kurt Soschinske and Dr. Bayram Yildirim for being part of the committee.

I would like to thank my parents and my family members for their constant support and encouragement, without them my education wouldn't be possible.

Finally, I would also like to thank Library Staff for their help, all my friends and colleagues in Computational Mechanics Laboratory at National Institute of Aviation Research for their support and cooperation.

ABSTRACT

According to National Highway Traffic Safety Administration (NHTSA), each year about 400,000 trucks are involved in motor vehicle crashes. Eighteen percent of these accidents are in rear-end crashes of the trucks. Accordingly, fatal injury had resulted to 5 percentages of the injuries. Whiplash is the common neck injury in rear impact consuming billions of dollars in insurance. However due to relatively low number of deaths or injuries in rear impact crashes, NHTSA does not conduct any rear impact testing to test the bumpers.

The main objective of this thesis is to study the effects of low speed impact on light trucks and the potential injuries on the occupants. The Federal Motor Vehicle Safety Standards (FMVSS) includes rear impact testing of fuel leakage, but only has a voluntary test for rear bumper impact test at low speed. In this thesis, the low speed rear impact simulation of a light truck was performed to understand the bumper deformation. A Chevy light truck is impacted to a flat barrier at 5 mph by using the finite element code LS-Dyna. This simulation is analyzed and validated for its bumper impact test.

A parametric study is thus performed to quantify the effect of various parameters on the rear end impact of the truck. Four vehicles were selected from public domain National crash analysis center (NCAC). These vehicles were Geo Metro, Chevy Truck, Ford Taurus and Ford single unit truck, selected according to the weight of the vehicles. The Chevy truck was chosen as target vehicle and other three models were selected as bullet vehicles. The target vehicle was then impacted with speed of 5, 10 and 15 mph. The accelerations were extracted from the center of gravity of the target vehicle (Chevy Truck). The acceleration pulses from the LS-Dyna were used in multibody analysis Mathematical Dynamic Model (Madymo). The seat model was built with similar characteristics as the Chevy truck seat. A Hybrid III dummy model was positioned with

seat and the model was given the acceleration pulses from the corresponding g's at low speed for the truck impacted at 5, 10 and 15 mph. This model was used to study the injuries on the neck. The developed model was then compared for neck response from the occupant with head restraint and without head restraint. Output of the dummy response resulted in injury values needed to be studied. The injury values were compared with standard critical values complying with injuries.

The result of this study can be utilized to obtain the effect of weight of impacting vehicles in low speed rear crashes of trucks. The impact response of the occupants and potential neck loads and injuries are also by products of this study.

TABLE OF CONTENTS

TABLE OF CONTENTS (Continued)

TABLE OF CONTENTS (Continued)

LIST OF TABLES

LIST OF FIGURES

LIST OF FIGURES (Continued)

CHAPTER 1

INTRODUCTION

1.1 Background

In the real world, the vehicles get impacted in different types of motor crashes and the occupants of motor vehicles are injured and killed crashes with varying directions. The crash between the two vehicles cannot be same; so many motor vehicle accidents involve more than one type of impact event. There are four different categories in which the vehicle impact events are widely classified; they are frontal, side, rear, and rollover.

Each type of associated crash has different probabilities of the crash event, different distributions of crash severities, and different patterns, causes, and risks of injuries for a given type of vehicle and/or mode of transportation. In the United States, side and rear impacts are the second and third most common type of vehicle impact, respectively after frontal impacts that result in injuries to occupants. Frontal crashes constitute more than 50 percent of serious and fatal injury-producing passenger motor-vehicle accidents; these types of crashes have been given the highest priority in establishing Federal Motor Vehicle Safety Standards (FMVSS). Side impacts account for approximately 27 percent of motor vehicle crash fatalities and 30 percent of motor vehicle crash injuries. Rear impacts account for approximately 5 percent of motor vehicle crash fatalities, a quarter of motor vehicle crash injuries, and are associated with serious medical consequences and significant societal costs. Each year about 400,000 trucks are

involved in motor vehicle crashes. Eighteen percent of the trucks are involved in rear-end crashes by Fatality Analysis Reporting System (FARS).

1.2 Rear Impact Crash

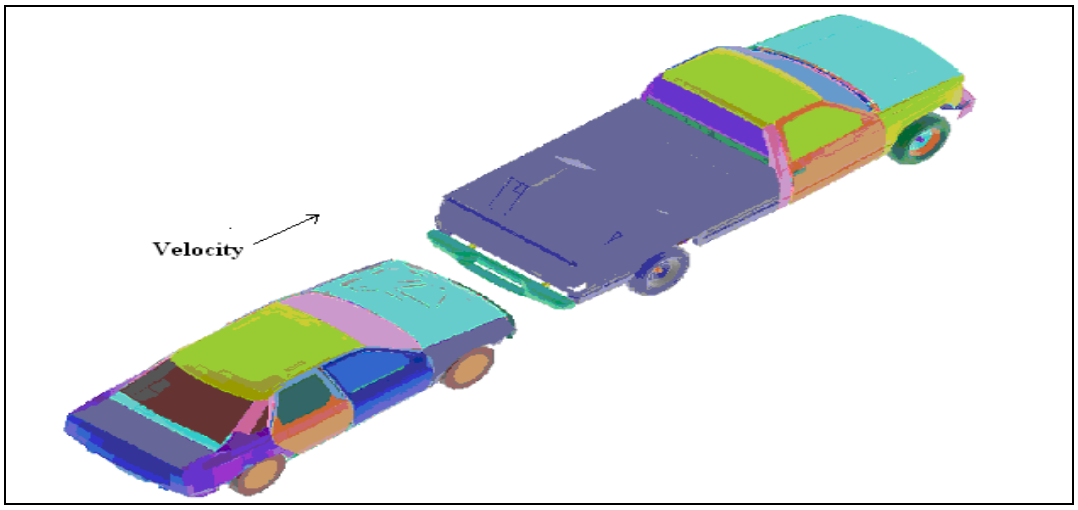

Figure 1.1. Rear Impact situation.

Nearly 95 percent of the 11 million vehicles involved in motor vehicle crashes in 2004 were passenger cars or light trucks (including pickups, vans, and utility vehicles with a gross vehicle weight rating of 10,000 pounds or less) 2004 Motor Vehicle Crash Data from FARS and the General Estimates System (GES). Figure 1.1 shows the rear impact situation, in which the truck is impacted by medium size vehicle. A pickup truck is defined as a light truck with a low-sided open body. In USA, pickup truck has become increasingly popular vehicles. Its use for personal transportation has attributed to increase in trends in pickup truck from 27.7 million registrations in 1987 to 36.2 million in 1997 was. Pickup truck had higher death rates than cars for single vehicle crashes, but because of their mass, they had lower death rates for multiple vehicles crashes (Evans, 1994) by

Insurance Institute for Highway Safety (IIHS). Several occupant safety concerns are raised with the use of Pickup trucks. Pickup and other light trucks have required meeting the most FMVSS applied to passenger cars National Highway Traffic Safety Administration (NHTSA). Drivers of the pickup truck had 60% use of the restraint compared to the 72% for passenger vehicles. These light weight commercial vehicle show in Figure 1.2 features a

1) A separate cabin

2) Rear load area or compartment

Figure 1.2. A typical pickup truck (wikipedia, 2004)

The compact pickup is the most widespread form of pickup truck worldwide. It is built like a mini version of a two-axle heavy truck, with a frame providing structure, a conventional cab, a leaf spring suspension on the rear wheels. The rear impact is the most common type of auto accident with approximately 2.5-million rear impact collision per year.

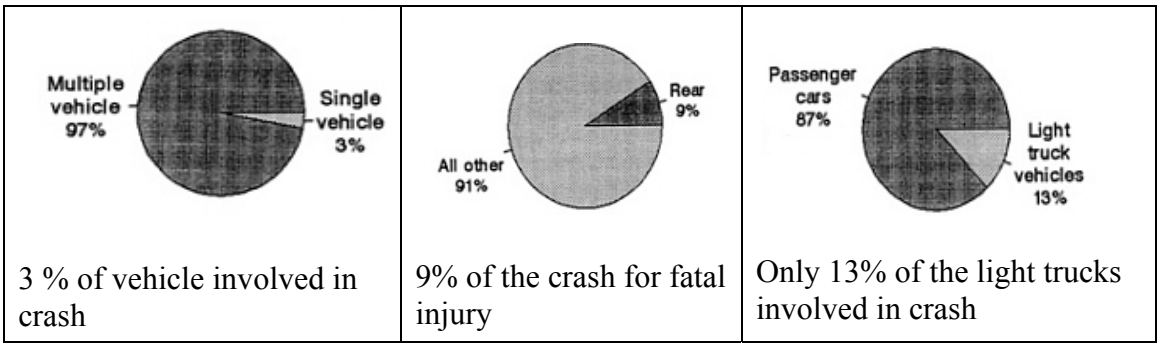

3 % of vehicle involved in crash	9% of the crash for fatal injury	Only 13% of the light trucks involved in crash

Figure 1.3 Vehicle involvements in fatal and rear impact crashes (NHTSA, 1999)

Vehicles involved in rear impact crashes account for 9 percent of the vehicles in fatal and injury crashes. According to Crash reports by NHTSA shown in Figure 1.3, the fatalities in rear impact are only 9 percent and crashes due to light trucks are only 13 percent.

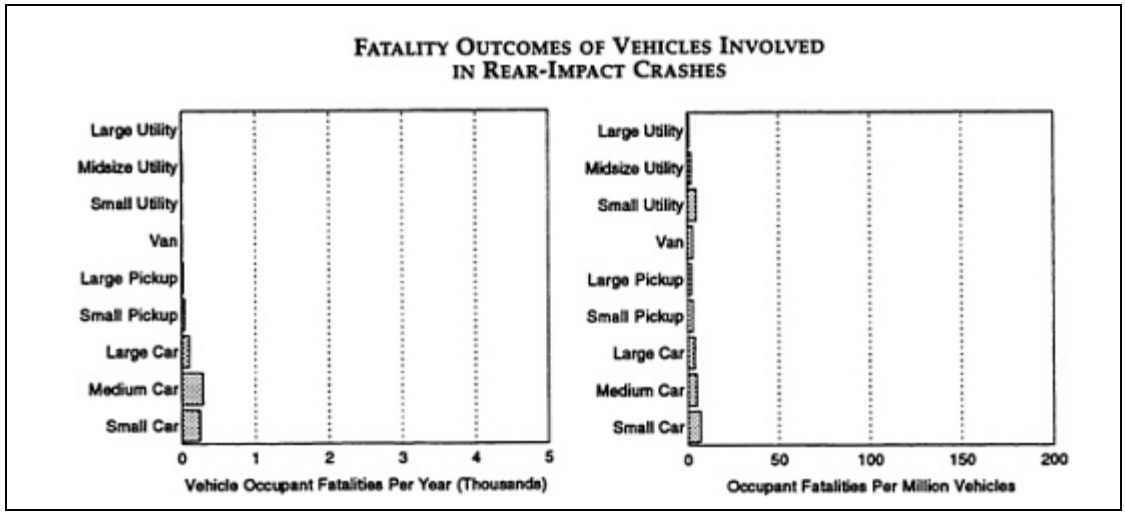

Figure 1.4. Rear impact crashes Statistics (NHTSA, 1999)

Also, in rear impact crashes, vehicle crash occupant fatalities per year are show in Figure 1.4, where the medium car has the highest vehicle occupant fatalities per year.

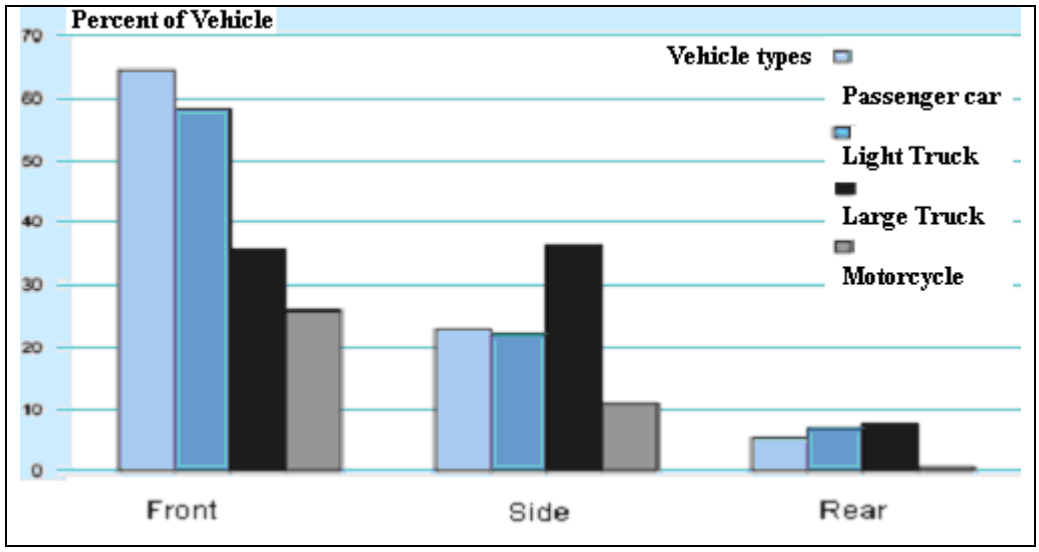

Figure 1.5. Percent of vehicles in crashes by initial point of impact and crash type (motor vehicle crash data, 2004)

The graph from the Figure 1.5 shows that 8 percent of the Light Trucks and 6 percent of the passenger cars are involved in initial point of impact in rear crash. A study called "The Cost of Highway Crashes" (Ted Miller et al, 1991) conducted for the Federal Highway Administration (FHWA) determined the economic losses associated with highway fatalities and injuries. The study by Ted Miller concluded that the average highway death costs $2.63 million and the average highway crash injury costs $44,000. There are 4.83 million injuries caused by highway crashes annually, 2 million are not medically treated while nearly 500,000 require hospitalization. Averages of 500-passenger vehicle occupants are killed and over 18,000 are injured each year in rear impact crashes with trucks. Based on the FHWA study's cost estimates, rear impact crash fatalities create economic losses exceeding $1.3 billion annually and injuries result in nearly $8 billion lost each year.

1.3 Rear Impact Injuries

The most common injuries with rear collision are related to back and neck injury. Whiplash is the most common injury caused by sudden flexion and extension of the neck. Neck injuries are reported at all impact speeds by (Jacobson, 1997) and (Otte et al, 1997). From accident research as well as tests with volunteers, it is shown that people sustain neck injuries frequently even in impacts with very low severity (Olsson et al, 1990), (Morris et al, 1996), (Siegmund et al, 1997). The U.S. NHTSA has reported during 1995 on 5.5 million of American people involved in a traffic accident. Subsequent studies showed that 53% of them have suffered from whiplash injury. The economic cost of whiplash has been estimated at roughly $4.5 billion per year in the United States. These types of injury can be expected to increase with use of cell phone and other distraction feature being added by automobile. IIHS, USA, has reported that whiplash occurs mainly due to poor head restraints and automobile seats.

1.4 Head Restraint

In a 1957 study, a head restraint design was proposed to minimize neck injury. The study proposed that a padded 6-inch fixed head restraint be attached to the top of automobile seat backs for neck protection. The General Services Administration (GSA) Standard 515/22 Head Restraints for Automotive Vehicles went into effect in October of 1967 for vehicles purchased by the federal government. It required that the head restraint be adjustable to 27.5 inches above the H-point and be between 1 and 4 inches behind the torso line. Restraints are rated as good, acceptable, marginal, or poor. The measurements

are made with a dummy representing an average-size male at a typical seatback angle. Head restraints have improved since the surveys began. Distance from the head restraint for average males head is shown in Figure 1.6. In 1995 only 3 percent of measured head restraints rated good compared with 45 percent in 2003. These ratings are a good indicator of the proportion of motorists likely to be protected in a rear-end crash

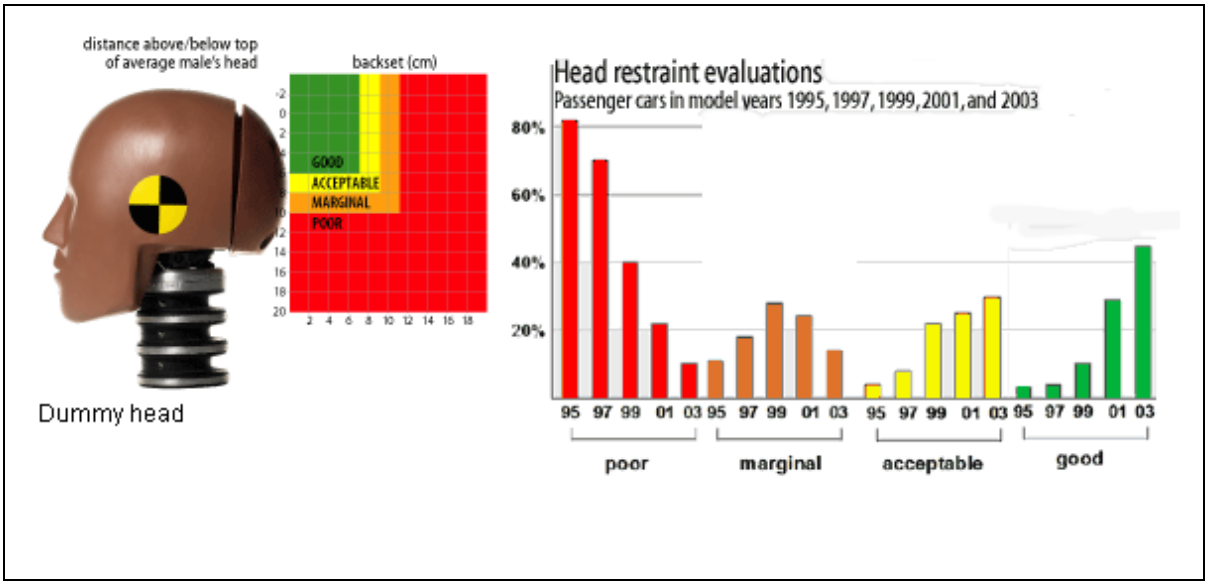

Figure 1.6. Backset distance from head with head restraint evaluations (NHTSA, 2004)

1.5 Whiplash

Whiplash and whiplash-associated disorders (WAD) are terms used to describe a range of neck injuries that are related to sudden distortions of the neck. The most common symptom whiplash victims report is pain due to mild muscle strain or minor tearing of soft tissue. Other injuries include nerve damage, disc damage, and in the most severe cases, ruptures of ligaments in the neck and fractures of the cervical vertebrae.

Much research into this type of injury following rear end crashes has been conducted during the last decade and many of the myths and concerns have been dispelled (Barnsley et al. 1998). Whiplash injuries are common in all types of crashes, motorists involved in rear-end crashes are more likely to experience whiplash. When a vehicle is struck from the rear it is accelerated forward, causing the seatback to push against the occupant's torso and propel it forward. The head lags behind the torso until the neck reaches its limit of distortion, then the head is suddenly accelerated by the neck much like the tip of a whip, hence the term whiplash. Head restraints limit the neck distortion that occurs before the head starts to follow the torso. The neck motion when subjected to rearward push the motion is extension and when it protracts, the motion is flexion.

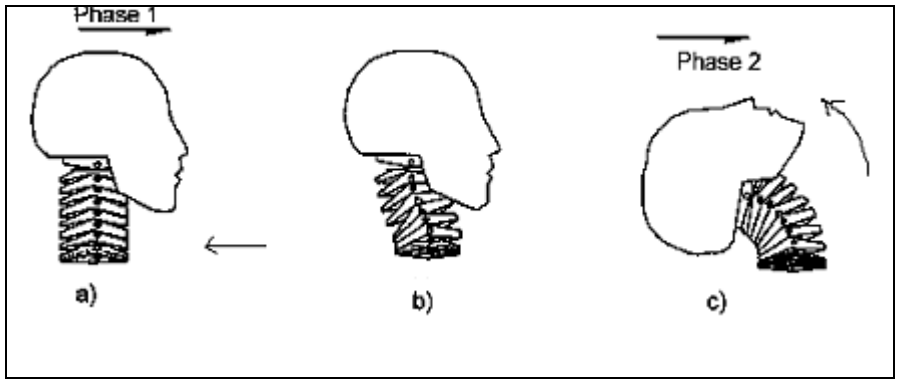

Figure 1.7. Extension of the neck in different phases (Svensson et al, 2000)

During a typical rear end collision the struck vehicle is subjected to a forceful forward acceleration. The head is subjected to a swift rearward translational motion followed by an extension motion. Figure 1.7 shows the neck movement of the head, in which the head extends backwards, is the extension motion.

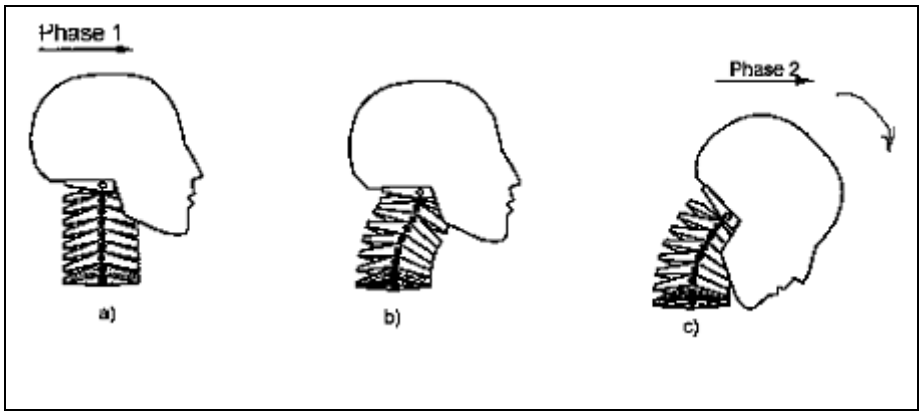

Figure 1.8. Flexion of the neck in different phases (Svensson et al, 2000)

At a later stage the head and torso will rebound forward and hit the seat belt, flexing the neck. The head rotates towards front in clockwise rotation as shown in Figure 1.8 with forces acting from the back of the head.

1.7 Injury Biomechanics

Biomechanical injury Due to impact load, human body experiences mechanical and physiological changes. Biomechanical response from such an impact can go beyond recoverable limits, resulting in damage to anatomical structure and altering the altering the normal function. The mechanism involved is called injury mechanism; the severity of the resulting injury is indicated by the expression “injury severity”. An injury parameter is a physical parameter or a function of several physical parameters that correlates well with the injury severity of the body region being examined. These scales rate the injuries instead of the results of the injuries. The most widely accepted anatomical scale is the Abbreviated Injury Scale (AIS). The AIS allow its application also for other injuries such

as burns and penetrating injuries. The AIS distinguishes the following levels of injury shown in Table 1.1.

Table 1.1 AIS injury scale (TNO theory, 2003)

Injury Scale	Injury level
0	No injury
1	Minor
2	Moderate
3	Serious
4	Severe
5	Critical
6	Maximum injury (causes death)
9	Unknown

The Abbreviated Injury Scale (AIS) provides researchers with a simple numerical method for ranking and comparing injuries by severity and to standardize the terminology used to describe injuries. AIS are shown in Table 1.2. The AIS are a "threat to life" ranking (MADYMO manual theory, 2003), numerical values have no significance other than to designate order. Biomechanical tolerance is the magnitude of a biomechanical response of the human body due to an impact that causes a defined level of injury. Most injury criteria are based on accelerations, relative velocities or displacement, or joint constraint forces.

Table 1.2 AIS Injury Categories

AIS	Category	Injury
1	Minor	Light brain injuries with headache, loss of consciousness, light cervical injuries, whiplash, and abrasion.
2	Moderate	Concussion with or without skull fracture, less than 15-minute unconsciousness, corneal tiny crack, detachment of retina.
3	Serious	Concussion with or without skull fracture, more than 15 minute unconsciousness without severe neurological damages.
4	Severe	Closed and shifted or impressed skull fracture with severe neurological injuries.
5	Critical	Concussion with or without skull fracture, more than 12 hours unconsciousness with hemorrhage in skull.
6	Survival not sure	Death partly or fully damage of brain stem or upper part of cervical with injuries of spinal cord.

These quantities must be requested with standard output options. Most injury criteria need some mathematical evaluation of a time history signal. Although originally intended for impact injuries in motor vehicle accidents, the updates of the AIS allow its application also for other injuries such as burns and penetrating injuries.

1.7 Injury Criteria

An injury criterion can be defined as a biomechanical index of exposure severity, which indicates the potential for impact induced injury by its magnitude. Most injury criteria are based on accelerations, relative velocities or displacements, or joint constraint forces.

The following injury parameter calculations are available

a) Gadd Severity Index (GSI)

b) Head Injury Criterion (HIC)

c) Neck Injury Criteria (FNIC)

d) Neck injury predictor (N_{ij})

The main injuries considered for rear impact are discussed

1.7.1 Neck Injury Criteria (FNIC)

Peak forces and moments in the upper and lower neck often assess neck injury. EEVC Working Group 111 has proposed a set of injury criteria, the Neck Injury Criteria. The element FNIC is used in order to discriminate with the NIC criterion for rear impact neck injury assessment that is based on the motion of the head relative to the thorax. (MADYMO manual theory, 2003) The FNIC is a measure of the injury due to the load transferred through the head/neck interface. The FNIC consists of three components

- the neck axial force,
- the fore/aft neck shear force and
- the neck bending moment about a lateral axis at the head/neck interface.

The FNIC injury calculation is applied to joint constraint load signals (Madymo manual theory, 2003). It is assumed that the coordinate systems of this (bracket) joint are oriented in agreement with SAE J221/1 because as axial force, the component of the constraint force in the joint z-direction is used, as fore/aft shear force, the component of the constraint force in the joint x-direction is used and as bending moment, the component of the constraint moment about the joint h-axis is used. Duration curves of these time history signals are made; the neck bending moment must not exceed 57 N-m.

1.7.2 Biomechanical neck injury predictor (Nij)

The biomechanical neck injury predictor, N_{ij}, is a measure of the injury due to the load transferred through the occipital condyles. This injury parameter combines the neck axial force Fz and the flexion/extension moment about the occipital condyles M_y.

Injury calculation is applied to joint constraint load signals (Eppinger et al, 1999). It is assumed that the coordinate systems of this bracket joint are oriented in agreement with SAE J221/1 because as axial force, the component of the constraint force in the joint z-direction is used, as shear force F_x, the component of the constraint force in the joint direction is used and as bending moment, the component of the constraint moment M_y about the joint h-axis is used. N_{ij} is the collective name of four injury predictors corresponding to different combinations of axial force and bending moment

- tension-extension (N_{te}),
- tension-flexion (N_{tf}),
- Compression-extension (N_{ce}), and
- Compression-flexion (N_{cf}).

The equation (1.1) for the calculation of Nij is given by

$$N_{te} = \frac{F_z}{F_{zc}} + \frac{M_y}{M_{yc}} \quad \text{.....(1.1)}$$

Where F_{zc} and M_{yc} are constants that depend on the dummy and on the neck loading condition (compression/tension and flexion/extension). F_z is the axial load and M_y is the extension moment of the neck. The sum of all predictors may not exceed value of one. For the case of tension-extension injuries, the axial tension load F_z is normalized with respect to critical value for tension F_{crit}. Extension moment M_{ext} is similarly normalized with respect to critical value of extension M_{crit}. Critical values for calculating N_{ij} are uniquely defined for each specific dummy size. The normalized neck tension-extension criterion is given by equation (1.2) as sum of these two normalized loads.

$$N_{te} = \frac{F_z}{F_{cric}} + \frac{M_{ext}}{M_{cric}} \quad \text{.....(1.2)}$$

Where F_z and M_{ext} are the axial force and extension moment calculated at the occipital condyles, respectively. F_{cric} and M_{cric} are the normalizing critical values for the force and moment, respectively (Eppinger R et al, 2000) for AIS 3+ injuries. According to the risk analysis published by NHTSA to support the supplemental notice of proposed rulemaking (Eppinger et al, 1999), an N_{te} of 1.0 was estimated to represent a 30 percent risk of AIS 2 neck injury, a 22 percent risk of AIS 3 injury, an 18 percent risk of AIS 4 injury, and a 7 percent risk of an AIS 5 injury. NHTSA has not updated these injury risk estimates. Risk assessments for the other load configurations (N_{tf} ,N_{ce} ,N_{cf}) are not available because the data set on which Nij is based does not include them. Another

analysis of the neck injury risk associated with an N_{te} value of 1.0 suggests a much lower risk of AIS 3+ neck injuries for subjects tensing their neck muscles in anticipation of a crash.

1.8 Modes of Injury

Most prominent injury modes are Tension-Flexion injury, Tension-Extension Injury, Compression-Flexion Injury, Compression-Extension Injury (MADYMO theory, 2003). In tension flexion injury, forces resulting from inertial loading of the head-neck system can result in flexion of the cervical spine while it is being subjected to a tensile force. Tension extension Injury is a combination of tension and extension of the cervical spine is the most common injury, which involves the soft tissues of neck and pain, is believed to reside in joint capsules of the articular facets of the cervical vertebral. In compression-flexion Injury forces acting on posterior-superior quadrant of the head, the neck is subjected to combined load of axial compression and forward bending. Frontal impacts to head with neck in extension will cause compression-extension injuries

Table 1.3 Critical neck injury values.

Neck Tension Extension	N_{te}	1
Neck Tension Flexion	N_{tf}	1
Neck Compression Extension	N_{ce}	1
Neck Compression Flexion	N_{cf}	1

The neck injury predictor (N_{ij}) values for hybrid III 50^{th} percentile male dummy are shown in Table 1.3. The injury can be predicted, if the value of N_{ij} is greater than 1.The head restraint position can play important part in designing seat.

CHAPTER 2

LITERATURE REVIEW

2.1 FMVSS for Rear Impact

A review of statistics of the rear end trucks shows that there is need for more research on rear end crash scenario to analyze crash mechanism and occupant kinematics. (Carl L.Ragland, 1998) studied the FMVSS 214 barrier impacting the rear of the subject vehicle to evaluate the fuel system integrity. The tests were conducted in two phases. The first phase examined rear impact test configuration differences such as overlap, speed and alignment; the second phase examined the performance of various vehicles using a consistent test protocol based on the first phase of testing and crash data analysis. With the overlap of 80 percent, moving deformable barrier at 80 mph impacted the Ford Mustang as shown in Figure 2.1. Amount of fuel leakage recorded was within the limit of FMVSS 301.

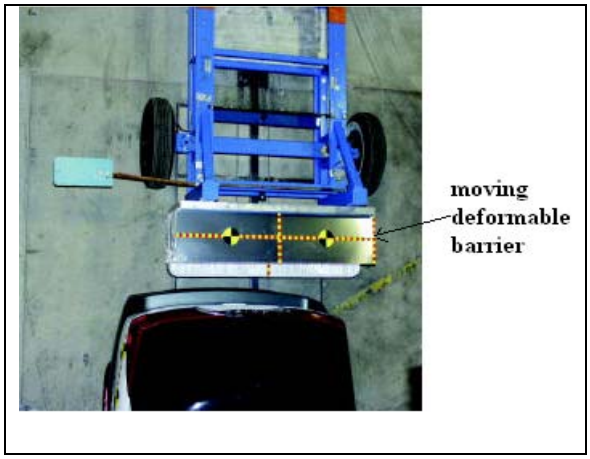

Figure 2.1. Deformable barrier impacting rear of passenger vehicle (mga corp, 2001)

The response of the driver and passenger Hybrid III anthropomorphic test devices (ATD) were taken, such as head and chest measurement and were compared with FMVSS 208 limits. The fuel integrity test only examined amount of fuel spillage in physical testing of a rear impact. The test did not study the rear end structure i.e. bumper deformation. Bumper performance standards are set by legislation at 5-mph for passenger cars; currently there are no bumper performance standards for light trucks. The governing design condition for a bumper system is 5-mph low speed impact requirement.

2.2 Bumper Performance

In the United States the National Highway Safety Transport Administration (NHTSA) has a standard for passenger cars that involves a series of car-to-barrier tests as well as pendulum (NHTSA, 1977). Tests, both of which were conducted at 5 mph. There were also pendulum impacts on the corners of the bumpers at 1.5 mph. There was no damaged allowed to other parts of the vehicle, although there was no limit to the damage to the bumpers and their attachments. The IIHS standard is a consumer information scheme. It involves low speed testing and was designed to evaluate bumper performance based on the cost of vehicle repair following four test configurations. The tests are conducted at 5 mph (8 km/h) and are full-width front and rear impacts into a flat barrier, a front impact into an angled barrier, and a rear impact into a centered pole. The first two are similar to the federal full-width impacts, whereas the latter two represent conditions encountered in the real world. The most widely accepted damageability test is from the Research Council for Automobile Repairs (RCAR) and aims to evaluate how easily and cheaply the damage can be repair. This procedure consists of two tests at 15 km/h; the

first is a 40 percent overlap front impact into a rigid barrier angled at 10 degrees, and the second is a 40 percent overlap rear impact by a 1,400 kg mobile barrier with the car again angled at 10 degrees. (Avery m, 2006) revealed that bumper beam was the key feature in determining the severity of the damage to the vehicles in low speed impacts. The geometry of the bumper beam determines its ability to maintain alignment between the underlying crash structures, which influences its ability to protect vulnerable areas of the vehicle. Examples of the geometry of vehicle pairings resulting in underride and override are shown in Figure 2.2.

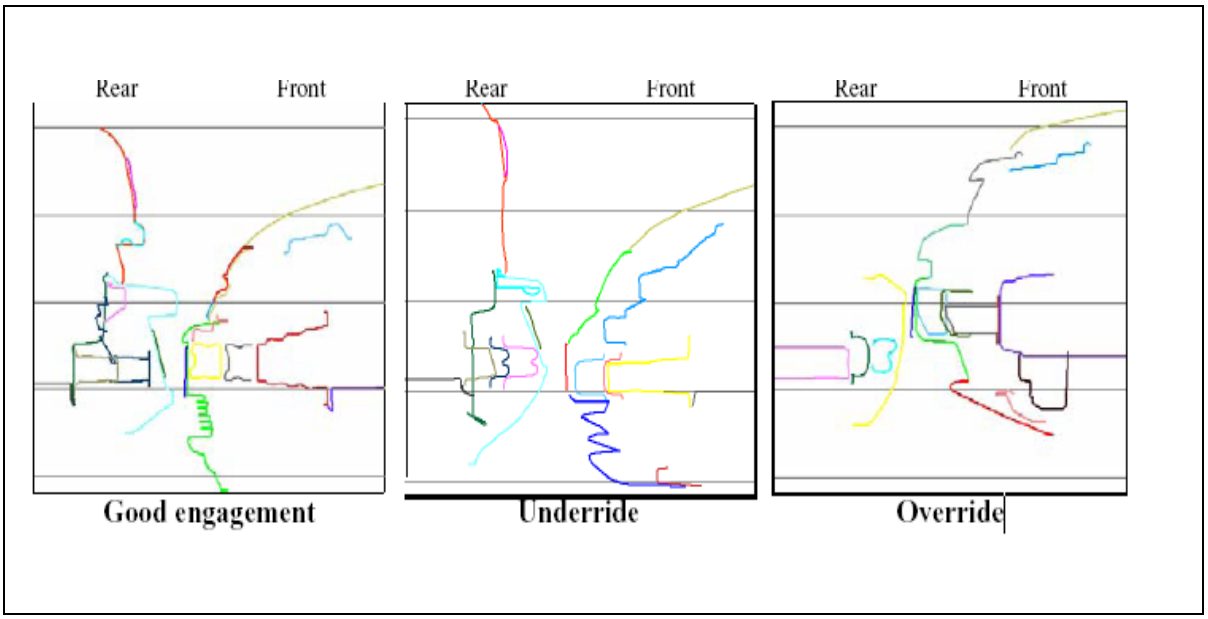

Figure 2.2. Cases of good engagement, underride and override. (Avery M, 2006)

In some vehicle pairings the overlap between the bumpers beams was very small, and override/underride tended to occur. This resulted in the highest damage and highest repair costs, and was particularly evident in the SUV to passenger car impacts.

(Heinrichs B .E, 2001) compares the damage to pickup truck produced by vehicle to barrier and vehicle-to-vehicle collision of similar severity. Five pickup trucks were subjected to barrier impacts and vehicle-to-vehicle impact on both their front and rear bumper speed, damage and high-speed video were recorded for each test. Impact force was recorded for barrier test. The average crushes obtained in barrier and vehicle showed significant correlation between barrier and vehicle crush values.

2.3 Comparisons of Hybrid III Dummy Models

(Derosia J et al, 2003) conducted rear impact sled test using 5^{th}, 50^{th} and 95^{th} percentile Hybrid III dummies to evaluate proposed injury criteria. Each dummy was placed on a standard automotive seat with head restraint mounted to a deceleration sled. The distance between the head restraint and back of the dummy was preset to zero, 50 or 100 mm, termed as backset different head restraint heights (750,800 mm) and backset positions were used to determine axial and shear forces, bending moments and injury criteria (NIC, N_{ij} and N_{km}). As shown in Figure 2.3, N_{ij} values for 5^{th} female, 50th male

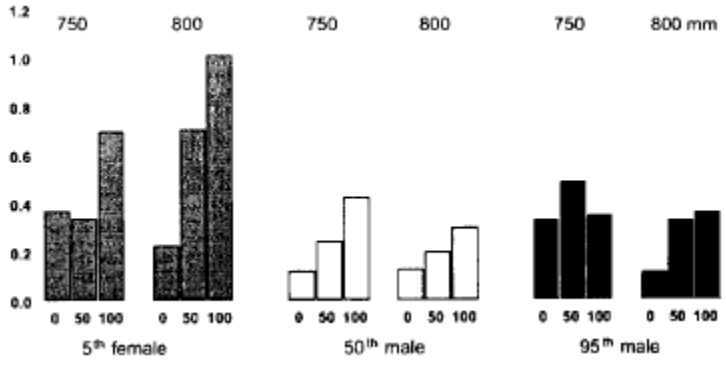

Figure 2.3. Injury criteria N_{ij} for 5^{th}, 50^{th} and 95^{th} percentile Hybrid III dummies (Derosia J et al, 2003)

and 95th male were compared for increasing backset distance. Head rotation increased with increasing backset and increasing head restraint height. Nij and N_{km} did not exhibit such clear trends. The 50th percentile dummy responded with consistent injury criteria values. None of the test exceeded the suggested injury criteria value of 1. Several types of dummies are available to study the rear impact response. Hybrid III, TRID, varying modifications of BioRID.The principle reason for choosing the Hybrid III is its availability and its mandate in US government for crashworthiness assessments. In addition, this dummy has good reproducibility characteristics.

(Butala K, 2004) studied the different rear end scenarios and its effect on neck injuries. The study compared the Neck Injury Criteria value for different impact scenarios.

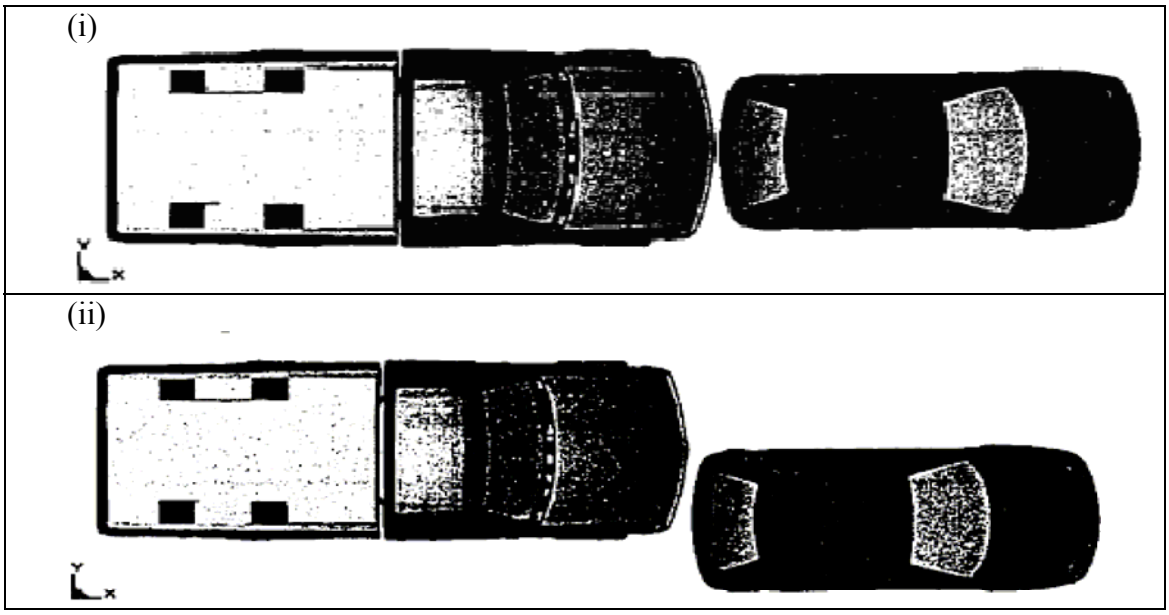

Figure 2.4. (i) inline impact (ii) offset impact (Butala K, 2004)

Geo M Finite element models, Ford Taurus and Chevy pickup were selected as target vehicle and Metro was impacted with these vehicles with three different crash situation viz inline, offset and angled rear end impact as show in Figure 2.4 and Figure 2.5. For Each scenario, the relative velocity was varied from 5-mph, 10-mph and 20-mph. Acceleration pulse was extracted from accelerometer at the center of gravity of the seat.

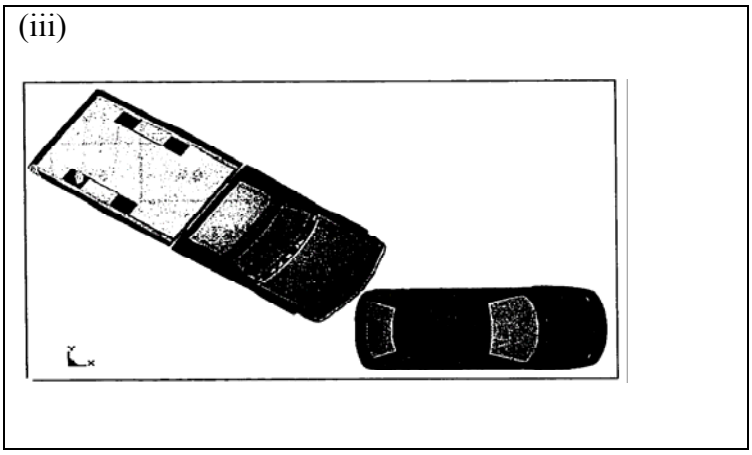

Figure 2.5. Oblique impact (Butala K, 2004)

Geo metro interior is modeled in MAthemetical DYnamic Model (MADYMO). Two dummies Rear Impact Dummy 2 (RID 2) and Biofidelic Rear Impact Dummy II (BIORID II) dummy were used to compare for its neck injuries in rear impact. Comparisons were done for neck loads, moment and N_{ij}.It was found that RID 2 facet dummy response was better compared with BIORID II dummy.

(Kleinburger, 1999) uses the computational modeling approach to better understand the effects of head restraints on the risk of cervical injury under rear impact condition. The height and backset were varied over a wide range, while engineering parameters were related to cervical injury risk. MADYMO dynamic simulations using a

human surrogate the approximate size of a 50” percentile male with sophisticated neck properties demonstrated that an increase in head restraint height from 27.5 to either 29.5 or 31.5 inches above the seating reference point substantially reduced loads on the cervical spine and thus may reduce the risk of neck injury during a low speed rear impact. For a head restraint height of 31.5 inches, the relative rotations, relative displacements, tensile loads, shear loads, bending moments, N_{te} values and NIC values were relatively low for backsets of about 2 inches or less.

2.4 Motivation

FMVSS 301 rear impact test gives the standard fuel spillage comparison and compares the head and chest measurement for ATD.Regulation does not consider the low speed impact on the rear of the vehicle.

Considering the neck injury in low speed rear impact, whiplash is the condition in which sudden extension and flexion of the neck occurs. An injury limit of the Hybrid III dummy model for low speed impact has not been studied for different g’s acting on the model.

(Butala K, 2004) had studied the comparisons of the Nij of RID 2 and BIORID 2 for different scenarios of rear impact. Hybrid III dummy model had not been used to study the neck injury criteria for low speed impact.

Study by (Kleinberger, 1999) considers the effect of head restraint on the Hybrid III dummy for different head restraint height and backset distance, but the study did not study the effect of head and cervical spine on Hybrid III with no head restraint.

2.5 Objectives

The objectives of this study are mainly to:

- Develop a validated finite element model for documented impact studies.
- Study the crashworthiness response in conditions involving different vehicle such as small car (Geo Metro), medium car (Ford Taurus) and large truck (Ford single unit truck).
- Analyze the effect of the weight and size of bullet vehicles on the target vehicle (Chevy truck) by comparing the accelerations.
- Study the occupant neck response and kinematics of Hybrid III dummy model for the seat model build in MADYMO, considering the seat with head restraint and without head restraint.
- Compare Nij for the Hybrid III dummy model for different weights in different seat condition with head restraint and without head restraint.

CHAPTER 3

BASCIC ANALYSIS SOFTWARE USED FOR STUDY

FMVSS demand stringent safety performance requirements for motor vehicles manufactured worldwide. These requirements focus on occupant safety and avoidance of severe injury. To ensure better product design and to be safety compliant, the automotive manufacturers conduct several physical crash tests. MADYMO rigid body and FE simulations help to reduce costs involved in physical prototype testing. Finite element method is used to obtain numerical solution of large engineering problems including stress analysis in dynamic condition. Mathematical models are used to apply on fundamental laws and principles of nature of the system. Numerical methods are used to solve complex problems in which exact solution is not possible. Finite difference method uses the differential equation for each node and derivatives are replaced for differential equation. This method is difficult to apply for complex geometries or non-isotropic material. Finite element method uses integral formulation to solve complex solution. There are lots of commercial codes available to solve steps in formulating equation. Finite element tools do the model analysis, these tools uses finite element method for numerical procedure that can be used to obtain solution to large class of engineering problems. These finite element tools are basic software used extensively in vehicles crashworthiness.

The following basic software that were used in the study of low speed rear impact are explained as follows:

3.1 EASi Crash DYNA (ECD)

EASi Crash DYNA is one of the powerful tools used in DYNA analysis developed by ESI group. ECD has good modeling and meshing features. It has good material database. It can assign material, define contacts and joints, and apply loads and boundary conditions in much better way. LS-Dyna is a complete, efficient and productive computer aided engineering environment for multibody and finite element occupant safety simulation.

3.2 LS-DYNA

LS DYNA is general-purpose finite element code for analyzing the large deformation dynamic response of the structures including structures coupled to fluids. The main solution is based on explicit time integration. LS-DYNA was built to handle the large deformations, sophisticated material models, and complex contact interactions required to analyze vehicle crash simulations. The material models used by LS-DYNA for this analysis include steel and aluminum, rubbers, foams, plastics, and composites. Additionally, LS-DYNA handles the complex contact conditions among multiple components and short-duration impact dynamics. LS-DYNA is used for all crash events frontal impact, side impact, rear impact, and rollover.

3.3 LS POST

LS-POST is the Postprocessor for LS-DYNA. The graphic user interface was carefully crafted to create a user-friendly environment. It has features such as plotting graphs, contours, vector plots, animation, SPH element generation and input deck manipulation.

3.4 EASi Crash MAD (ECM)

EASi-CRASH MAD, initially developed by EASi Engineering is a basic preprocessing tool that supports MADYMO.ECM facilitates in building 3D MADYMO models for CAE analysis and to post process the results. EASi-CRASH MAD is a unique pre and post processor tool, under a single user interface, which provides both graphical and XML editing features and currently supports MADYMO 6.2 and lower versions.

3.5 Madymo (Mathematical Dynamic Model)

Madymo is general-purpose code to simulate dynamic behavior of mechanical systems. It combines multi body techniques involving complex kinematics joints for simulation of kinetics of systems and also FE simulation techniques for structural behavior of systems. Madymo is uses to simulate crash situations to a higher degree of accuracy and to Asses injuries sustained by the victims.

3.6 MSC Patran

Patran is the leading pre- and post processor for CAE simulation. The program's advanced modeling and surfacing tools allow creating a finite element model from scratch. Patran imports model geometry without modifications. As a post-processor, Patran quickly and clearly displays analysis results in structural, thermal, fatigue, fluid, magnetic terms, or in relation to any other application where the resulting values are associated with their respective finite elements or nodes.

CHAPTER 4

MEHTODOLGY

In this chapter, from the objective of the study, the approaches to the methods are shown in steps. These steps are shown in Figures 4.1, 4.2 and 4.3 respectively and described in the following conditions.

Step I

Finite Element Model of Chevy from NCAC
Contact between the truck and rigid steel barrier is given in key file by Contact_automatic_surface
Distance between the bumper & rigid barrier is 300mm
Coefficient of friction between rigid plane and tyre part of truck=0.5
Velocity of 5 mph is given to part of truck

Step II

Finite Element of truck at 5mph

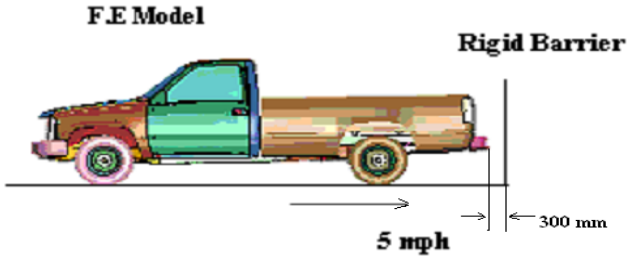

Step III

Validation of reduced Models from NCAC (reduced model) of Chevy truck for low speed bumper test.

Figure 4.1. Steps for validating model.

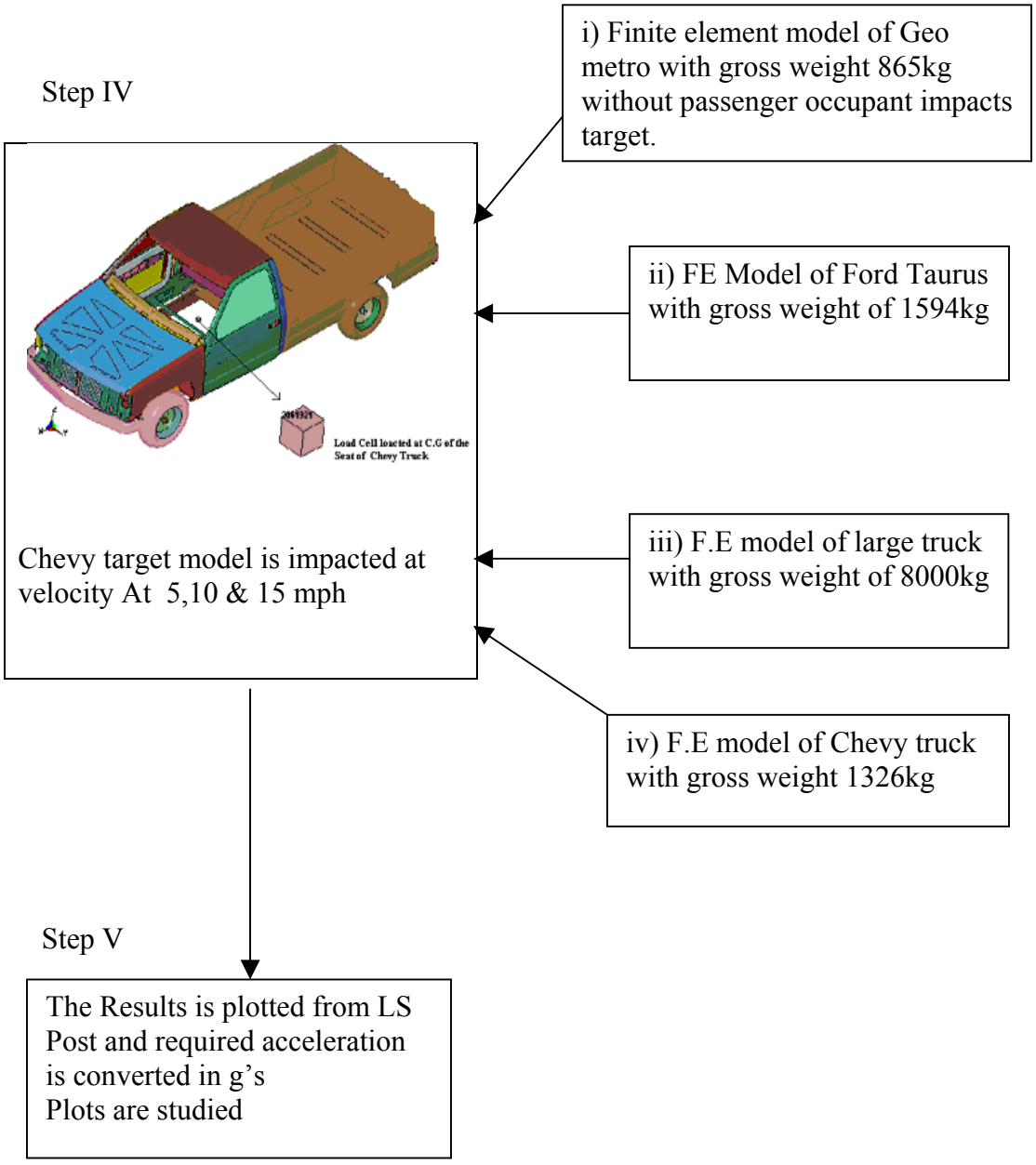

Figure 4.2. Steps to study low speed.

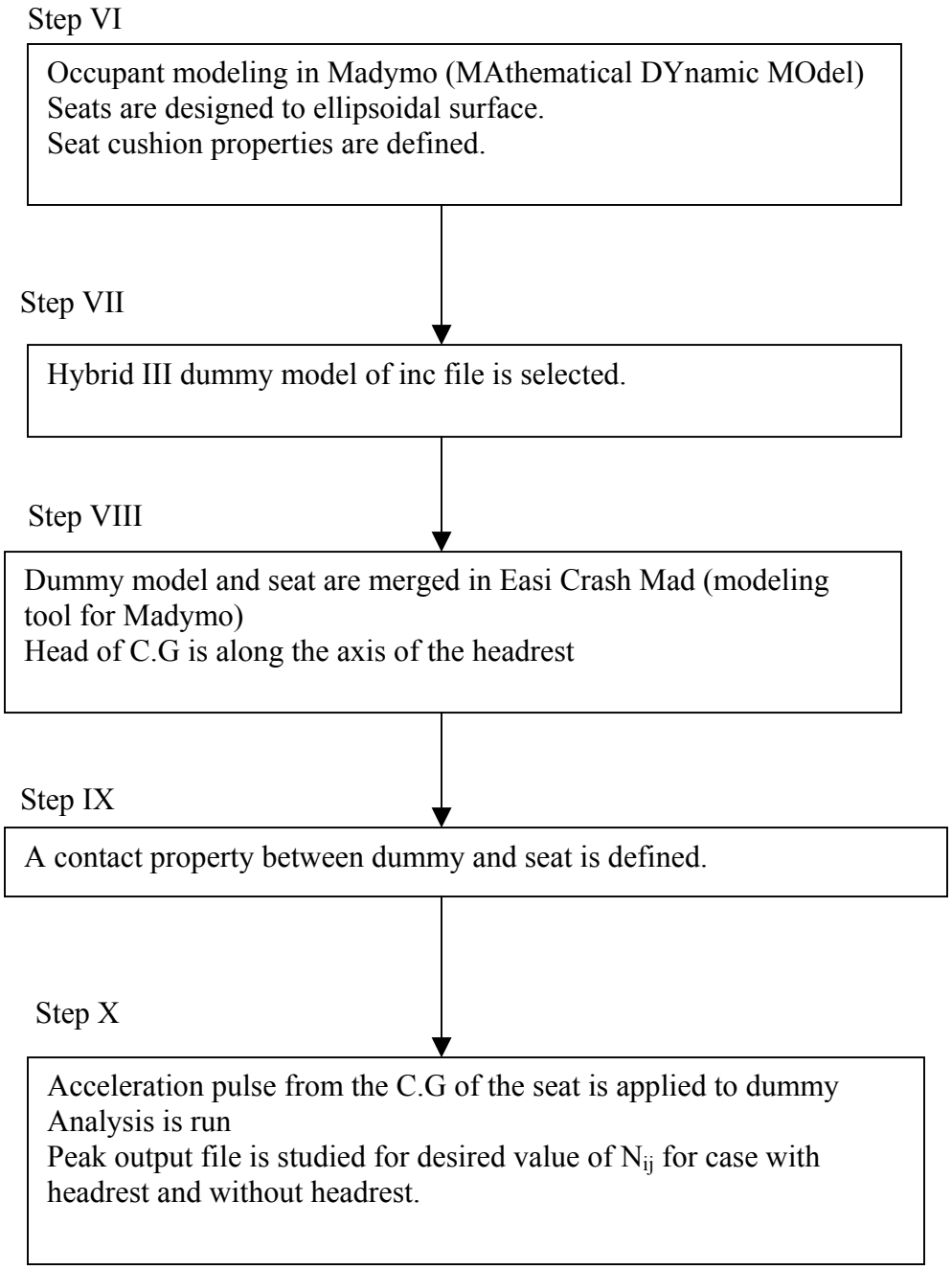

Figure 4.3. Steps to occupant response.

4.1 Structural Crash Dynamic Analysis

Following steps are used to study the low speed rear impact

4.1.1 Step I

The rigid barrier was needed for validation of model. MSC Patran was used to create the barrier. Geometric properties were defined with length of 1200mm; height of 600 mm. Surface was defined selecting the length and height of the rectangle. Using the mesh feature, mesh seeds were given to the rectangle. Surface was then extruded to the

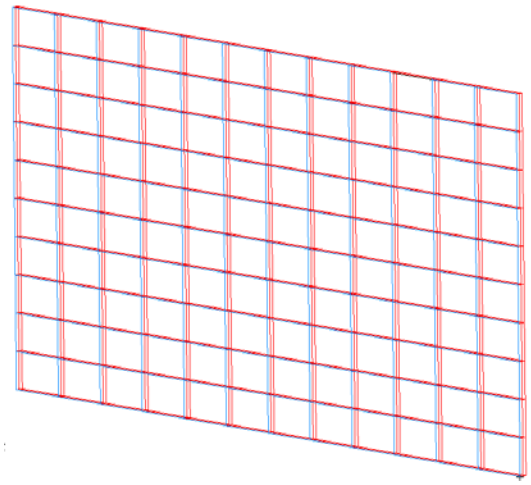

Figure 4.4. Elements of rigid barrier.

depth of 100 mm as shown in Figure 4.4. No of elements were 240.Meshing can be defined as the process of breaking up one large component into smaller elements in order to facilitate numerical solutions. Normally, surface domains are subdivided into triangular or quadrilateral shapes, and volume may be divided into tetrahedral or

hexahedral shapes. After meshing the rectangle, material properties were defined with density of 7.8×10^{-9} kg/mm^2, young's modulus of 2×10^5 N/mm^2 and poisons ratio of 0.3.Boundary condition were give to the bottom surface of the barrier. It was constrained in all directions. Finally the key file was generated with run analysis. The reduced model of Chevy truck in format of key file was imported from National Crash Analysis Center (NCAC) to ECD.Rigid plane was created in ECD using the command of 'RIGIDWALL PLANAR'. Contact between the Chevy truck and rigid wall were established by selecting the nodes of the wall as 'MASTER' and nodes of the tyres of the truck as the 'SLAVE'.

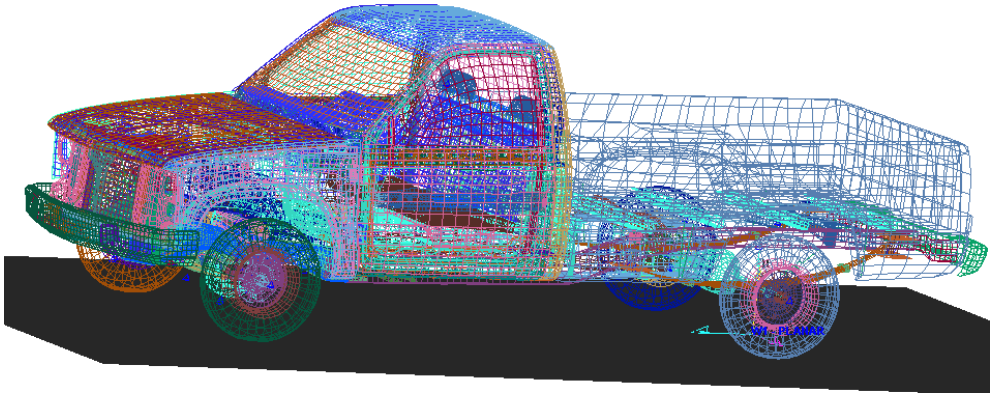

Figure 4.5. Rigid wall combined with Chevy truck

The key file of the rigid barrier was opened in ECD and combined with the FE model of the Chevy truck with rigid plane as shown in Figure 4.5.Two key files are combined to one key file and the nodes were numbered automatically while the Auto node feature was used to merge the two files. The combined key file was changed referring to Dyna manuals.

4.1.2 Step II

The distance between the rear bumper of the Chevy truck and rigid wall was kept at a distance of 300 mm. Distance between the two objects were kept minimum to reduce the simulation time of the analysis, which was run in LS Dyna.

The combined key file was changed by referring the card format from LS Dyna manuals Typical card format and its use in Dyna format is demonstrated

1) *CONTROL_TERMINATION

This card is used to define the termination time of the the analysis

*CONTROL_TERMINATION				
$# ENDTIM	ENDCYC	DTMIN	ENDENG	ENDMAS
1	0	0.	0.	0.

Simulation time was initially ran for 0.6 secs, which was later increase to 1 sec to get the desired results for the validation of the bumper.

2) *CONTROL_TIMESTEP

It is used to set the structural time step size control using different options

*CONTROL_TIMESTEP							
DTINI	TSSFAC	ISDO	TSLIMT	DT2MS	LCTM	ERODE	MSIST
0.	0.5	1.12E-06	-1.12E-06	0	0	0	

The scale factor for computed time step is set to 0.5 for the combined key file.

3) *MAT_RIGID

LS Dyna has over one hundred metallic and non-metallic material models like Elastic, Elastoplastic, Elasto-viscoplastic, Blatz Ko rubber, Foam models, linear

visco-elastic, glass model etc. Material properties for the bumper part were defined with the material ID 2000253, which was defined for the Part ID 2000253.

*MAT_RIGID							
$# MID	RO	E	PR	N	COUPLE	M	ALIAS
2000253	7.8E-09	200000.	0.3	0.	0.	0.	0.
$# CMO	CON1	CON2					
1.	0.	0.					
$# A1	A2	A3	V1	V2	V3		
0.	0.	0.	0.	0.	0.		

Material can be defined by defining density "RO", Young's modulus "E", Poisson's ratio "PR"etc. CMO, CON1 and CON2 are the constrained parameters.

4) *INITIAL_VELOCITY_GENERATION:

The card is used to define the initial translational velocity of the part ID

*INITIAL_VELOCITY_GENERATION						
$# SID	STYP	OMEGA	VX	VY	VZ	
2001858	1	0.	2235.5	0.	0.	
$# XC	YC	ZC	NX	NY	NZ	PHASE
0.	0.	0.	0.	0.	0.	0

Section ID 2001858 is defined by selecting all parts of the Chevy truck; velocity of the car is given at 2235.5 mm/sec i.e. at 5 mph. The necessary key file changes were done and the simulation was ran for 1 secs.

4.1.3 Step III

To validate the Chevy truck bumper for low speed at 5 mph, bumper deformation was observed in LS post.

4.1.4 Step IV and V

Finite element models of the bullet vehicles i.e. Geo metro, Ford Taurus and Ford single unit truck were obtained from NCAC.FE model of these vehicles are shown in Figure 4.6.Each model, which act as a bullet vehicle, was open in ECD and merged with the Chevy truck. Contact distance between the target and bullet model was kept at 300 mm. Distance was maintained between the rear bumper of truck and front bumper of the target vehicles.

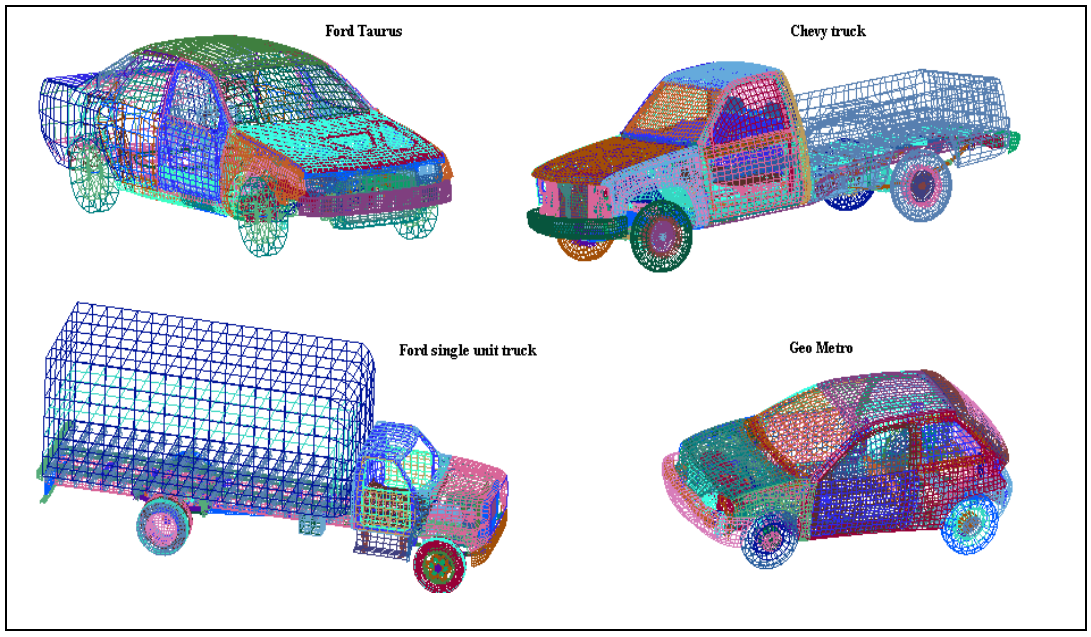

Figure 4.6. Different models used for impact.

The results of the Dyna file is opened in LS-Post, where graphs of acceleration of load cell at the node versus time can be found. The graphs taken from the LS-Post were compared for results.

4.2 Occupant Multibody Interaction Analysis

To study the occupant response following steps was used to design seat model and analyze injury values.

4.2.1 Step VI,VII and VIII

Easi Crash Mad (ECM) was used to model the seat in ellipsoidal surface. The interior of the car was imported in ECM 3.2.Vehicle model was loaded into the model window. Seat dimensions of the ellipsoidal seats are shown in Table 4.1.

Table 4.1. Ellipsoidal seat dimensions in mm.

Body name	A	B	C
B1	250	200	40
B2	50	180	300
B3	35	120	100

Seat model was made near the interior of the imported vehicle. The multibody car seat model has a seatback and seat bottom. The seat characteristics modeled included the sear back hinge stiffness, head restraint cushion stiffness and friction coefficient. Each part of seat is made of ellipsoid, which is shown in Figure 7.1. Each surface is defined by

defining its center of gravity, mass and inertial properties. The bodies were connected by fixed joint .The whole systems were connected with reference space by using free joint. The seat contains three ellipsoid as shown in Figure 4.7. These ellipsoids are positioned and oriented as per requirement. The seat back was modeled at 20 degree recline form the vertical. The head restraint was 6 inches in height, 12 inches in width and 5 inched in depth. The head restraint was repositioned parallel to vertical plane. Head restraint height was specified according to FMVSS 202 of 27.5 inches.

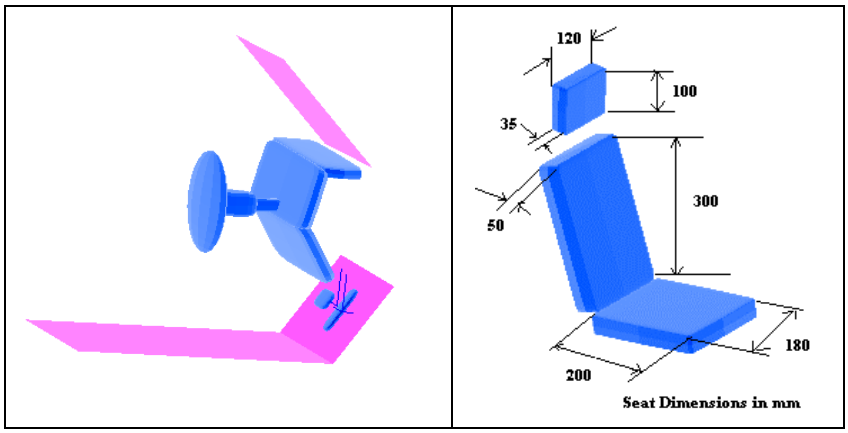

Figure 4.7. Car interior and seat dimensions in mm.

Hybrid III 50th percentile male dummy was used for the study of low speed was selected from standard dummy database. Hybrid III 50th percentile dummy is most widely used in automotive safety restraint system. Size and weight of dummy is average size and weight of the US population. It is accepted in several standards FMVSS 208, ECE R. 94 and used in global National Crash Analysis Program (NCAP).

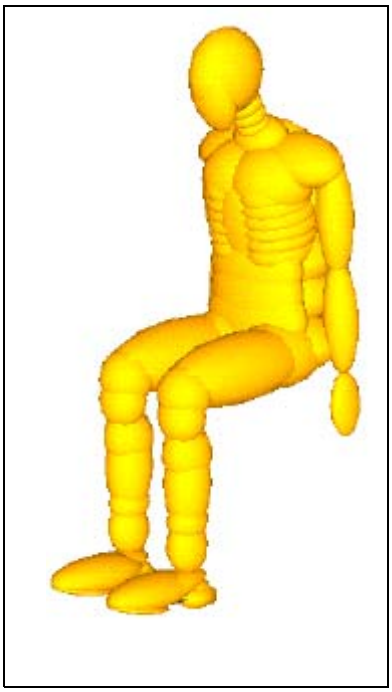

Figure 4.8. Hybrid III Dummy model (TNO Automotive, 2003)

It consists of 69 bodies, with 6 left and right ribs as shown in Figure 4.8. There are 5 kinematics joints representing the neck and the reference joint is chosen in lower torso. The inc file of the dummy was used to merge with the vehicle seat with interior. Dummy was positioned on the ellipsoidal seat by arranging the dummy head such that its center of gravity of the head is along the center of the head center of the head restraint.

4.2.2 Step IX and X

There are three types of contacts that can be defined in MADYMO:

1) (MB_MB) Multi-body-multi-body Contact (contact between two surfaces)
2) (MB_FE) Multi-body-Finite Element Contact (contact between a surface and element/nodes)
3) (FE-FE) Finite-Element-Finite-Element contact (contact between two surface)

MB-MB contact is defined between seats and hybrid dummy where the seat was treated as MASTER body and dummy as a SLAVE body. Friction coefficients used between the contacting bodies were 0.5 between dummy head and headrest, 0.7 between dummy back and seat bottom. Contact type was set to MASTER, such that the contact point is on the SLAVE and the characteristics of the MASTER were used. The acceleration pulse from Center of gravity of the Chevy truck was converted to SI units. The gravitational acceleration pulse was defined which acts in Z direction of the reference space. Figure 4.9 shows the graph of acceleration versus time. Acceleration pulse of -9.81 m/sec^2, i.e, 1 G acts downward on the dummy system.

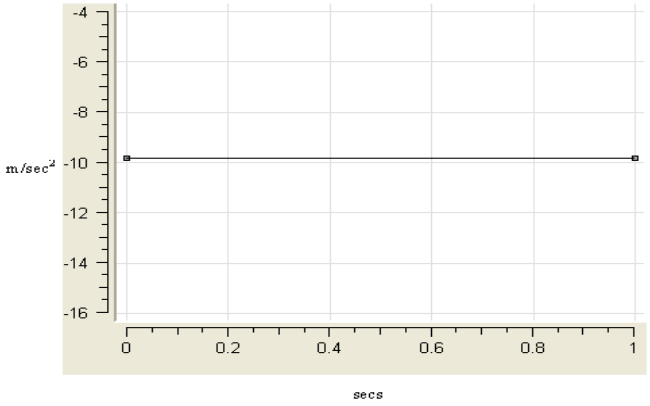

Figure 4.9 Acceleration pulse.

The whole system is connected with reference space using free joint. The pulse from different cases of rear impact is applied to dummy model in MADYMO. The input file of the model was saved and analysis was run to obtain the desired results. The required head kinematics of the dummy model was studied.

CHAPTER 5

VALIDATION OF THE FE MODEL

5.1 Chevy Truck Finite Element (FE) Model

The finite element model was taken from public domain developed by EASi Engineering for NHTSA studied by (A Zaouk et al, 1997). The FE model of Chevy Truck is shown in Figure 5.1.

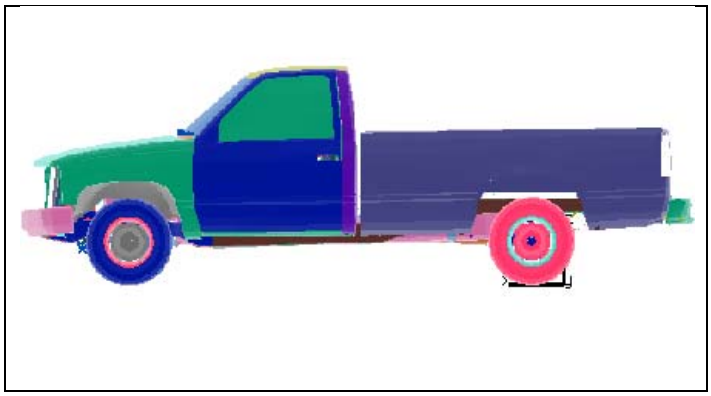

Figure 5.1. FE model of Chevy truck (Zaouk et al, 1997)

The vehicle model was divided in to 248 parts; these parts are the components of the vehicle as shown in Table 5.1. Two types of shell elements were used, they are quadrilateral and triangular. The material model assigned to shell element was general isotropic elastic-plastic material. The stress strain relation for isotropic elastic plastic material was defined with required stress strain points. The beam elements use the isotropic elastic material model. The contact and friction between the components were

modeled with one single surface-sliding interface also known as automatic contact for beam, shell and solid element worth arbitrary segment orientation.

Table 5.1. FE Components of truck

Number of Parts	**248**
Number of Nodes	**16050**
Number of Solids	**3561**
Number of Shells	**14028**
Number of Elements	**17850**
Weight (Kg)	**1236**
CG (mm) Rearward of the front wheel	**123**

5.2 Accelerometer

An Accelerometer is device used to measure velocity in different directions. Accelerometers are modeled to measure the acceleration at various locations. In this study the accelerometer was kept at the center of gravity of the seat. It was placed at a distance of 1230 mm from the rearward from the front wheel as seen in Figure 5.2. In a rigid body three nodes define the accelerometer, which defines a triad to measure accelerations in the local system. The presence of an accelerometer means that the accelerations and velocities of node 1 will be output to all output files in a local coordinate instead of global coordinates.

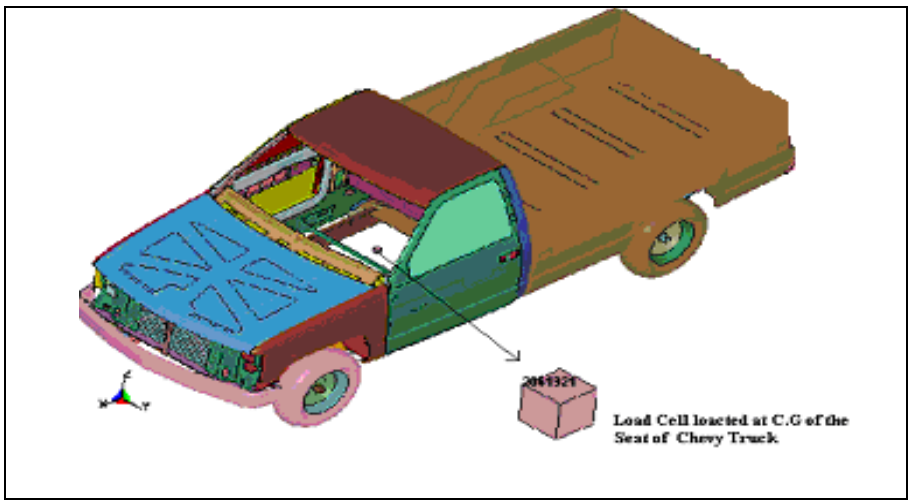

Figure 5.2. Location of Accelerometer.

The three nodes should be part of the same rigid body. The finite element model needed to be correlated against the test factor to validate the models use to simulate.

5.3 Finite Element Model Validation

The Finite Element Model of the Chevy Truck Obtained from NCAC Model is validated for its Bumper test. Validation is a process to check if criteria are correct with a set of standards. Data from full vehicle crash is taken to validate F.E Model. Currently there are no bumper standards. NHTSA (National Highway Traffic Safety and Administration) has been conducting voluntary bumper test at 2.5 mph for the light truck category. At these speed there should be no visual damage on a vehicle. However, full crash data from F.E model can be validated with Crash Test from Manufacturers. There are two full-scale tests that are full frontal and rear impact with the fixed barrier.

5.4 Rear Impact Bumper Test Validation

According to United Stated NHSTA (49 CFR) Part 581, Bumper standards state that at rear impact at 5 mph there shall be no visual impact. The set up of the FE Truck model was done according to test procedure. A 3000-pound Chevy truck was impacted to a fixed steel barrier. An FE simulation was conducted for 1sec and resultant data from the C.G of the truck was obtained. The Deformation at the bumper and the velocity of the load cell gives the required outputs. Vehicle kinematics in rear bumper test, as shown in Figure 5.3.

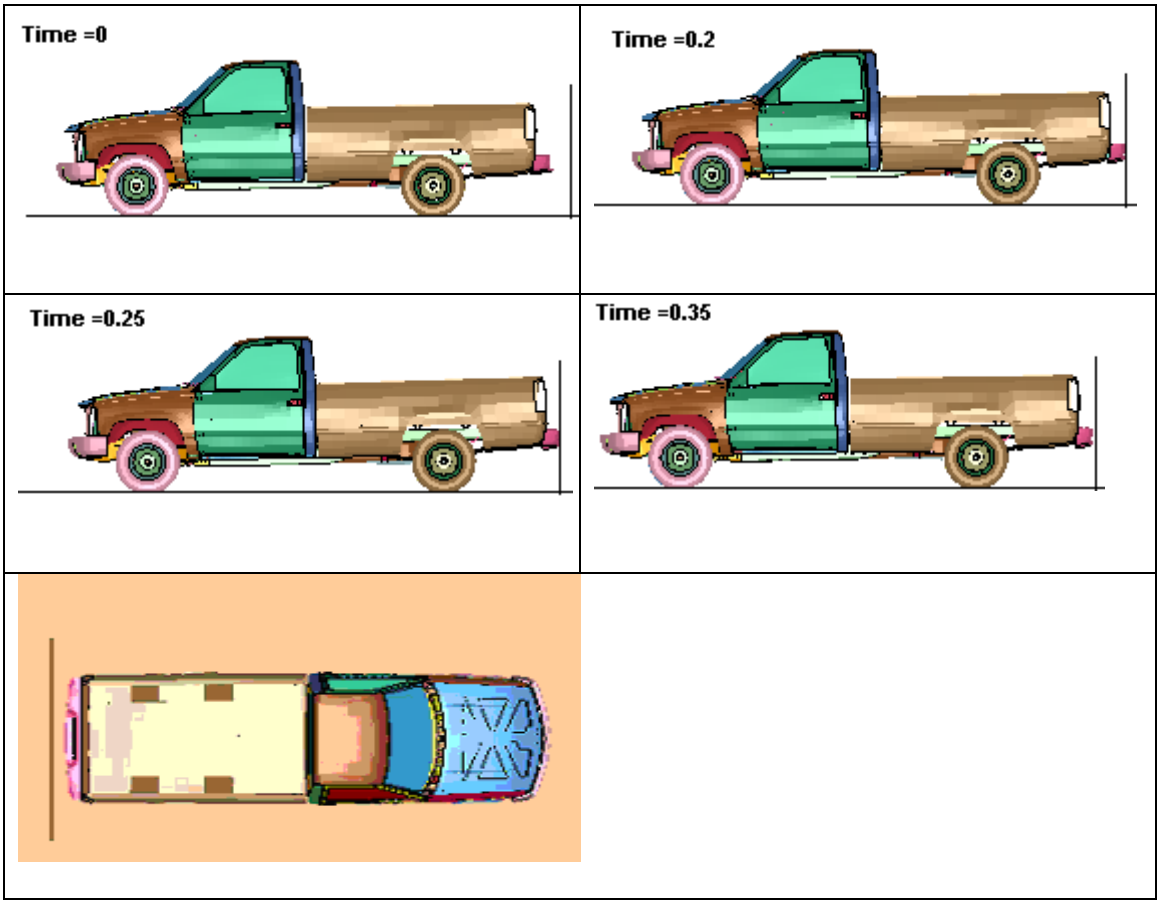

Figure 5.3. Shows the bumper impacting the rigid wall at different interval.

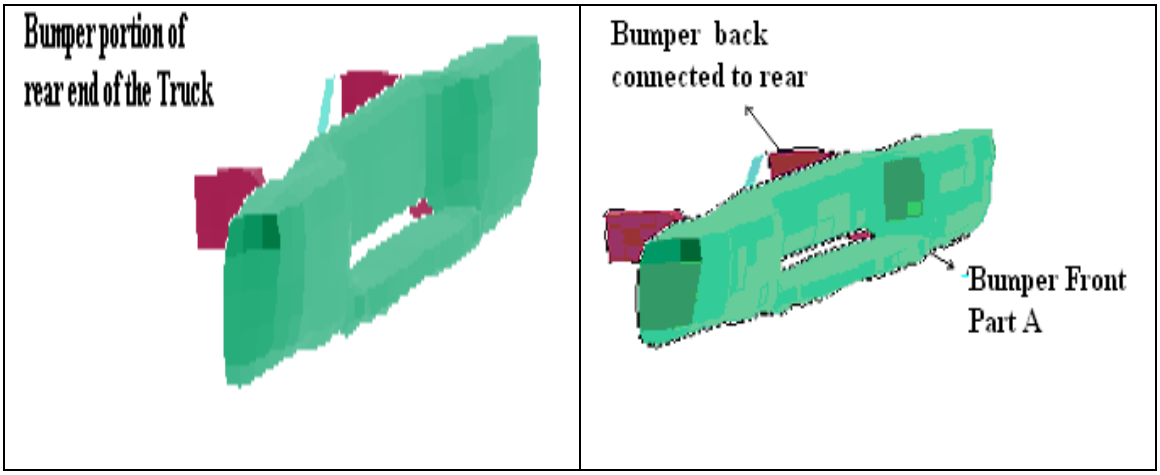

Figure 5.4. Bumper part of the rear of the vehicle

The bumper front part A is shown in Figure 5.4. The bumper is made of steel structure. Effect of the low speed impact at 5 mph on bumper shows the deformation pattern in Figure 5.5.

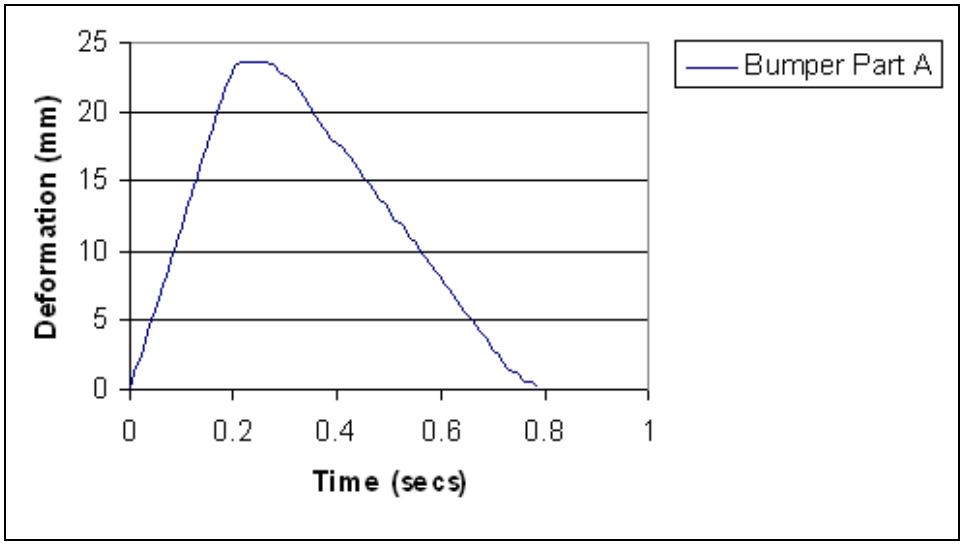

Figure 5.5. Deformation (mm) of the bumper part A to validate the bumper test.

For 0.24 secs bumper deformation of part A increases very rapidly due to contact of the barrier with flat rigid barrier. Deformation depends on material, stiffness, distance and type of contact. Bumper material of standard steel was used with yield strength of 270 N/mm^2. The deformation increases to 23.8mm.The material in bumper shows elastic behavior and the deformation decreases to zero.

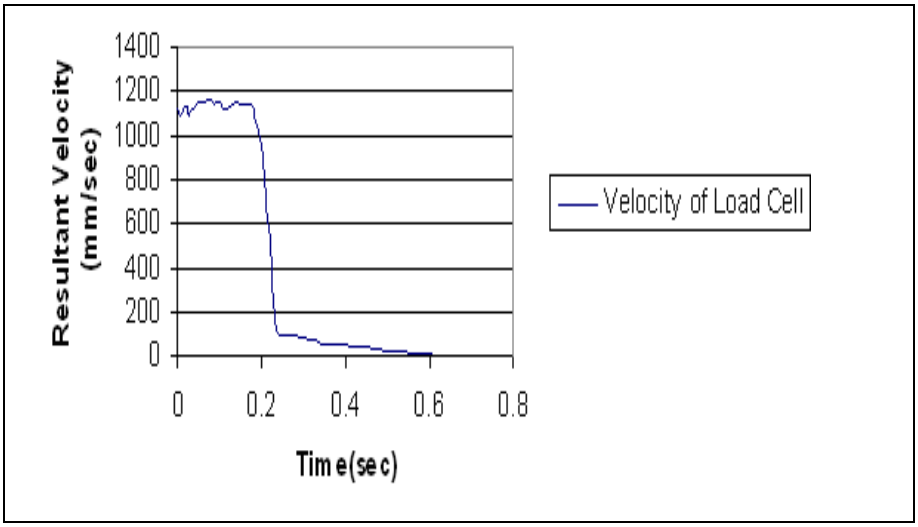

Figure 5.6. Resultant velocity versus time.

The resultant velocity of the node at the load cell of the C.G of the truck is shown in Figure 5.6. The velocity remains stable for 0.18 secs, decreases with after collision to 0.23 secs and it continues to stabilize till 0.6, after that truck comes to halt. The maximum velocity for load cell is 1180mm/sec. The contours of the bumper displacement are show in Figure 5.6. Bumpers shown visually clearly explain the elastic material behavior of the rigid bumper in the rear of the Chevy truck.

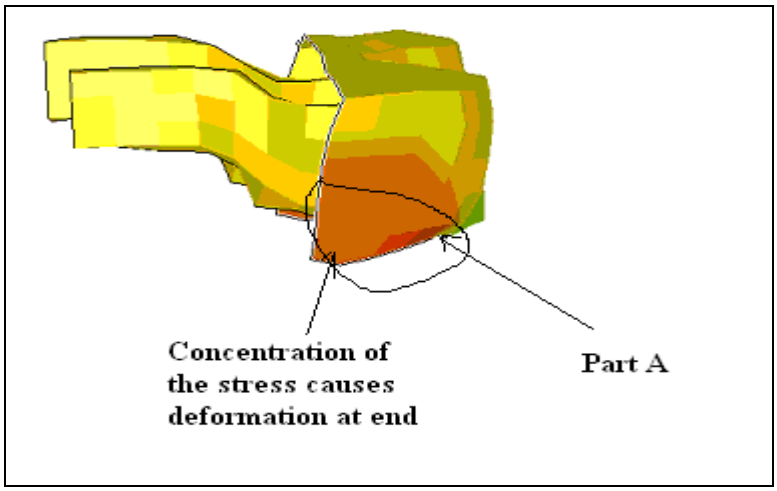

Figure 5.7. Bumper deformation.

Amount of stress concentration is more at the corner of the bumper as shown in Figure 5.7. Rigid wall remains intact and it does not move, producing equivalent force of impact on the rear bumper.

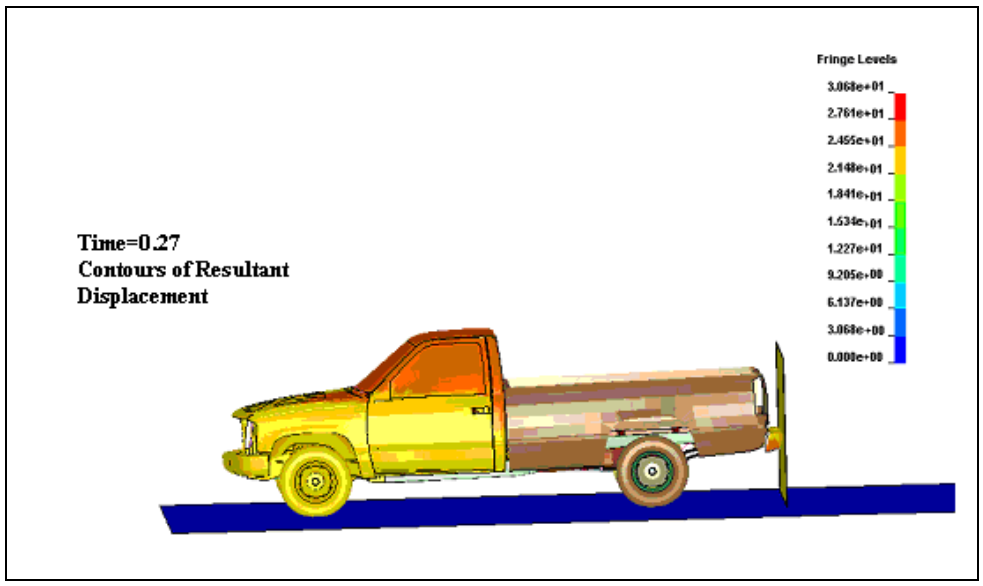

Figure 5.8. Contours of Displacement.

Contours of resultant displacement of bumper with rigid plane is shown in Figure 5.8.

To check the condition of deformation, the stress level of the rear bumper were measured. It was found that stress level did not increase the yield stress of the bumper. It can be assumed that bumper was not permanently damaged and regained its original shape. As soon as the bumper impacts, the material of bumper becomes elastic in nature and tries to reach yield strength of the material. But due to low impact speed material does not reached its yield strength and bumper regains its original shape due to elastic behavior in bumper material. Contours of displacement taken from LS-Post are shown in Figure 5.8 for time step of 0.27.The resultant graphs of deformation, velocity and displacement pattern shows that in low speed bumper test, there should be no visual damage. Amount of damage can only increase if the stress level of the bumper increases the yield strength of the material. From the simulation of the truck at 5-mph the bumper regains its original shape and validation criteria needed for the study of the deformation of the bumper is verified.

CHAPTER 6

ANALYSIS OF THE STUDY MODELS IN REAR IMPACT

A parametric study of various vehicles impacting the target vehicle is shown in Table 6.1.Rear bumper of the Chevy truck was inline with bullet vehicles. Frontal bumper of the bullet vehicles comes in contact with rear bumper of the target vehicle.

Table 6.1 Parametric studies of models in rear impact

Case	Bullet Vehicle	Target Vehicle	Speed of bullet vehicle at rear (mph)
1	Geo Metro	Chevy Truck	5
			10
			15
2	Chevy Silverado C-2500	Chevy Truck	5
			10
			15
3	Ford Taurus	Chevy Truck	5
			10
			15
4	Ford single unit large truck	Chevy Truck	5
			10
			15
			20

In case of rear impact analysis, four situations were studied, in which four different size and weight of the car, viz. Geo Metro, Ford Taurus, Large size pickup truck and Chevy pickup truck were used as bullet vehicle impacting target vehicle as Chevy truck.

6.1 Geo Metro (Sub Compact Car)

The Geo metro is a subcompact hatchback car. A detailed model was developed at NHTSA as shown in Figure 6.1.

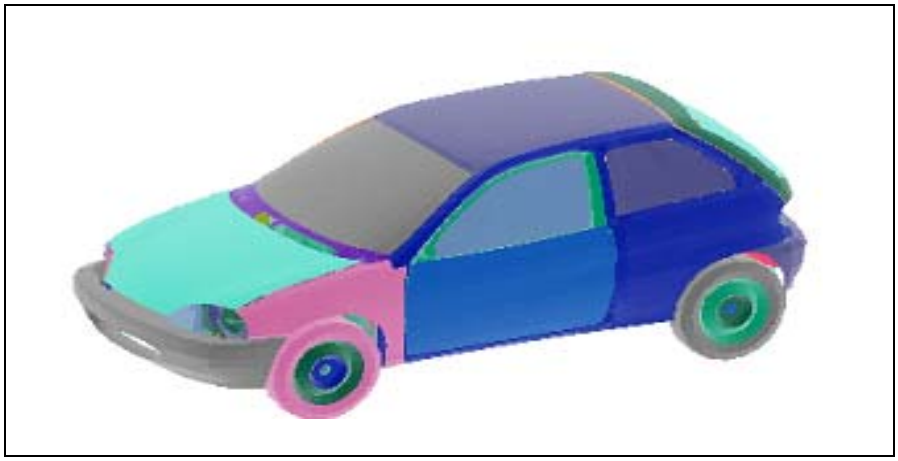

Figure 6.1. FE model of Geo Metro.

The vehicle components has 230 different parts. There are 20348 nodes, 1209 solids, 76 mass elements and 2 beam elements as shown in Table 6.2. Solid element use stress solid element or fully integrated element formulation theories, shell elements use Belytschko-Tsay shell theory. Solid elements are defined by either rigid material model or metallic honeycomb model while sheet metal parts are defined for isotropic elastic plastic material. The accelerometer is located at the Center of gravity of the seat at the distance of 884 mm rearward of the front wheel. The FE model is merged with the target vehicle. The whole body parts are defined to one PART name in key file.

Table 6.2 FE Component of Geo Metro.

Number of Parts	**230**
Number of Nodes	**20348**
Number of Solids	**1209**
Number of Shells	**18980**
Number of Elements	**19200**
Weight (Kg)	**865**
CG (mm) Rearward of the front wheel	**884**

The contact between the body parts of Geo Metro as bullet vehicle and Chevy truck as a target is specified under AUTOMATIC_SURFACE_TO_SURFACE contact type card. Established Part ID is given velocity by using INITIAL_VELOCITY_GENERATION for initial velocity to the bullet vehicle. Geo metro is used as a bullet or impact vehicle. The vehicle is impacted inline with target vehicle at low speed.

6.2 Ford Taurus (Mid-Size Sedan)

The vehicle FE model used for the simulation is based a 1991 Ford Taurus is shown in Figure 6.2. It was developed by EASi Engineering for the National Highway Traffic Safety Administration (NHTSA). Initially, the model was developed and validated for a frontal impact into a flat rigid wall; consequently the frontal portion of the vehicle was modeled in details while the center and rear of the portions were modeled with a coarse mesh or beam elements. Since the central and rear portions of the vehicle

do not undergo significant deformations in such impact, modeling these parts of the vehicle with coarse mesh or beam elements does effect the accuracy of the results as long a the overall mass distribution and inertia of the model are consistent with those of the actual vehicle.

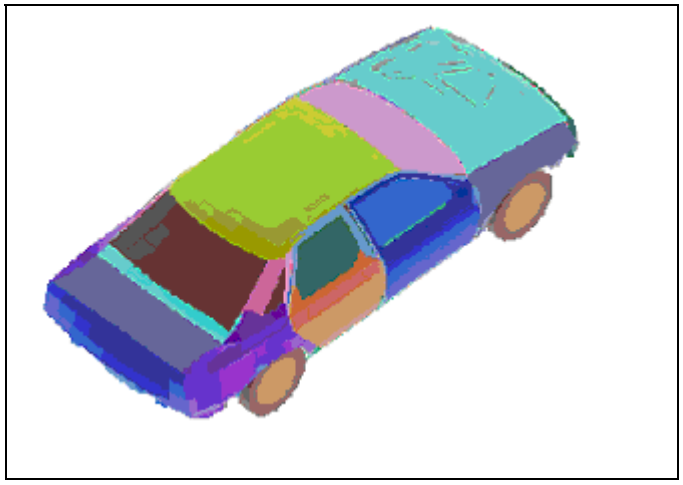

Figure 6.2. FE Model of Ford Taurus.

The vehicle model is subdivided into 133 parts. Each part represents a component in the vehicle. Out of the 133 parts, 104 parts are used with shell elements to model the sheet metal components, 18 parts are assigned beam elements to represent the steel bars in the vehicle along with some of the connections between the sheet metal components, and one part is used with brick elements to model the radiator as shown in Table 6.3. Two types of shell elements are used in the model, quadrilateral and triangular. The formulation for both shell types is based on the Belytschko-Tsay shell theory, which is the default shell formulation in LSDYNA3D. The material model assigned to these shell elements is a general isotropic elastic-plastic material (material type 24 in LS-DYNA3D).

Table 6.3. FE Component of Ford Taurus.

Number of Parts	**133**
Number of Nodes	**26793**
Number of Solids	**348**
Number of Shells	**27873**
Number of Elements	**28636**
Weight (Kg)	**1394**
CG (mm) Rearward of the front wheel	**945**

The stress-strain relation for the isotropic elastic-plastic material is defined with eight stresses versus strain points. The beam elements in the vehicle model are based on Hughes-Liu beam formulation and use the isotropic elastic material model (material type 1 in LS-DYNA3D). The solid elements, are assigned material type 26, metallic honeycomb, and use the constant stress solid element formulation. The FE vehicle model components are connected to each other using the spot weld and rigid body constraint options in LS-DYNA3D. The contact and friction between the components are modeled with one single surface sliding interface type 13; also known as automatic contact for beam, shell, and solid elements with arbitrary segment orientation.

6.3 Ford Single Unit Truck (Full size Truck)

The single unit ford truck is obtained from NCAC as shown in Figure 6.3.The model consists of 133 parts, 348 solids and 28636 elements. It is the one of the largest category of the full size trucks.

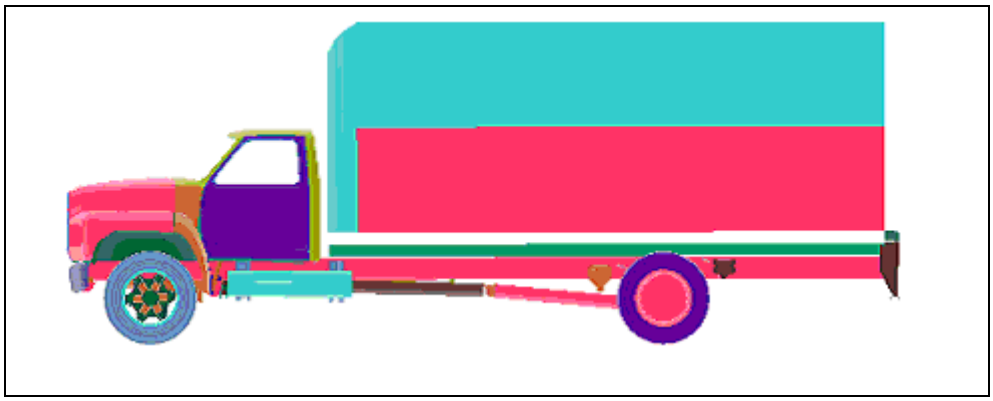

Figure 6.3. FE model of Ford F800 Single unit Truck.

The heavy truck weighs 8000 kg, which is 5 times more, then Ford Taurus. The load cell is located 1055 mm rearward from the front of the wheel.

Table 6.4. FE Component of Heavy Truck.

Number of Parts	**133**
Number of Nodes	**56793**
Number of Solids	**348**
Number of Shells	**57873**
Number of Elements	**58636**
Weight (Kg)	**8000**
CG (mm) Rearward of the front wheel	**1055**

The FE model of heavy truck was merged with target vehicle. The contact ID was given to bullet truck and Chevy truck as target. The velocity was given to the heavy truck and impacted with the target vehicle at low speed. The model obtained from NCAC is opened in EASi Crash Mad. The FE model of Geo Metro was merged with Chevy truck

and was placed at distance of 200 mm from the bumper. Geo Metro was impacted at low speed of 5,10 and 15 mph with the rear on Chevy truck.

6.4 Case (1) Impact speed of Geo Metro at 5, 10 & 15 mph

Impact of the low weight vehicle with the Chevy truck is as shown in Figure 6.4 in different time frames. Simulation starts at 0.0 secs, vehicle continues to move towards target vehicle with increasing time frame. Rear end Kinematics for Geo Metro (bullet vehicle) and Chevy truck (target vehicle) Small car contacts the vehicle at 0.15 secs. Impact speed of 5, 10 and 15 mph affects the Chevy truck. Account of bumper impact takes place with front bumper of small car impacting below the rear bumper of the Chevy truck.

It can be seen from the Figure 6.4 that the front bumper of Geo was below the rear bumper of the Chevy truck. In this vehicle pairing there was small overlap between the bumper beams. This overlap causes structural deformation of the parts above the bumper. This deformation increases with increase in speed of the vehicle There was some amount of incompatibility in the response from the target vehicle. Force of the small car is transferred to the truck by momentum principle. When the vehicle being struck was at rest, it had no velocity and, hence, no momentum. The bullet vehicle, that strikes a target vehicle, had a momentum based on its velocity and mass. As soon as the vehicle impacts the truck, the acceleration level recorded at the center of the gravity of the seat of truck increases for 0.3 secs.

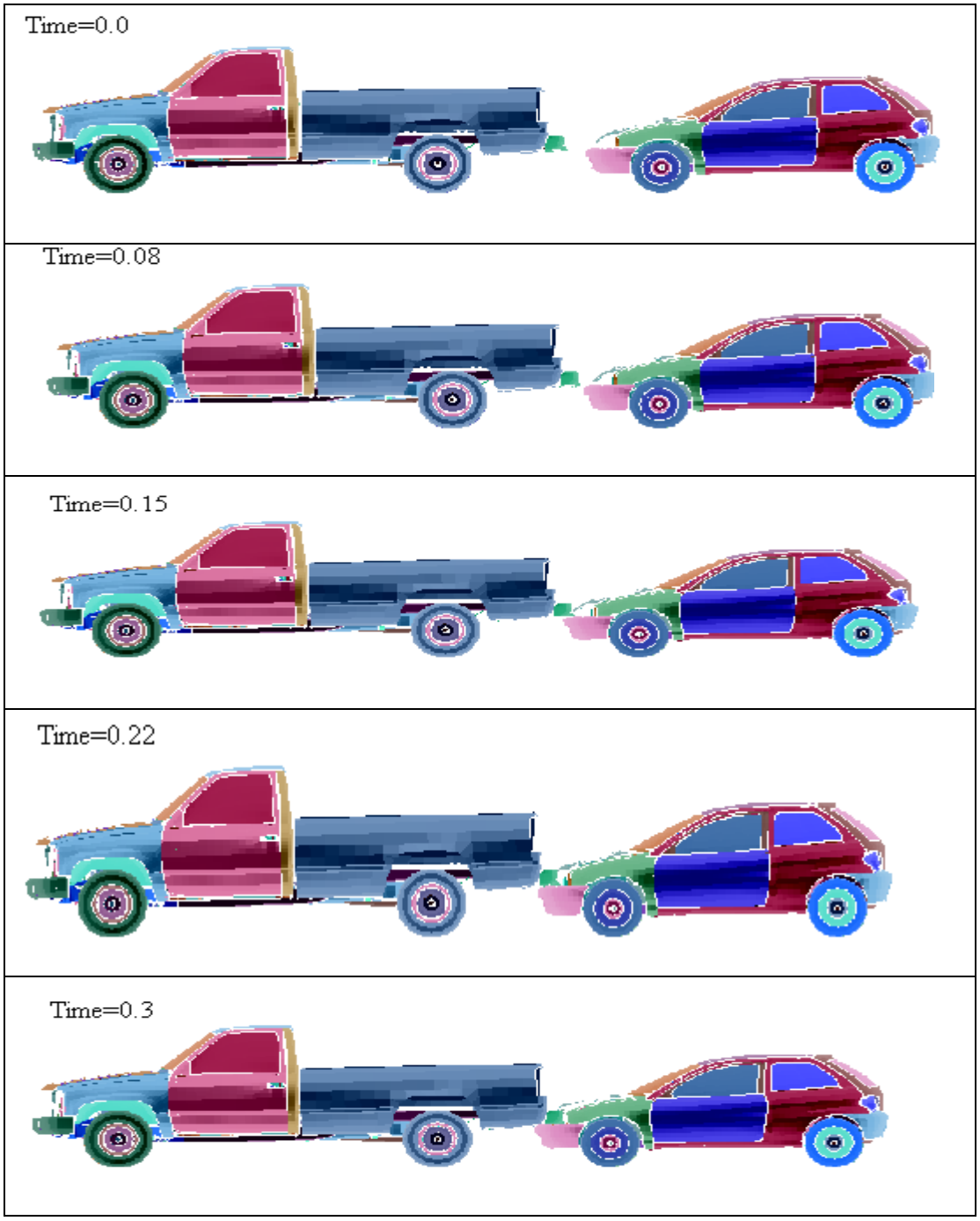

Figure 6.4. Simulation of low speed impact at 5mph.

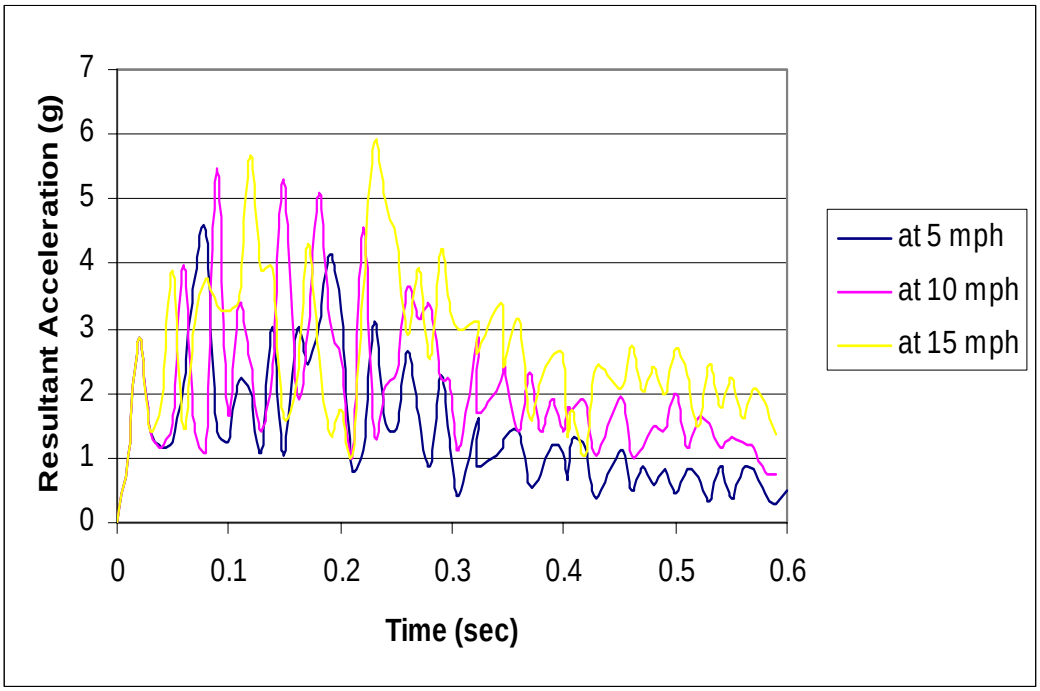

Figure 6.5. Resultant acceleration graphs from impact by Geo Metro.

As shown in figure 6.5, the acceleration level varies for different speed of impact. Effect of Relative velocities at low rear end and the maximum accelerations of the vehicle were observed. Acceleration reaches to 4.8 g for 5-mph and the 5.7 g for 10-mph. The acceleration levels reaches to 6 g for the 15 mph impact from rear. It reaches its maximum level at the end of the simulation time i.e. after 0.2 secs. The acceleration decreases once it reaches the maximum level. Acceleration can be seen to slow down, as at 0.6 secs the acceleration reaches below 1 g.

6.5 Case (2) Impact speed of Chevy truck at 5,10 &15-mph

Target vehicle is similar to the bullet vehicle and impacts at a distance of 300 mm from the rear end of the truck.

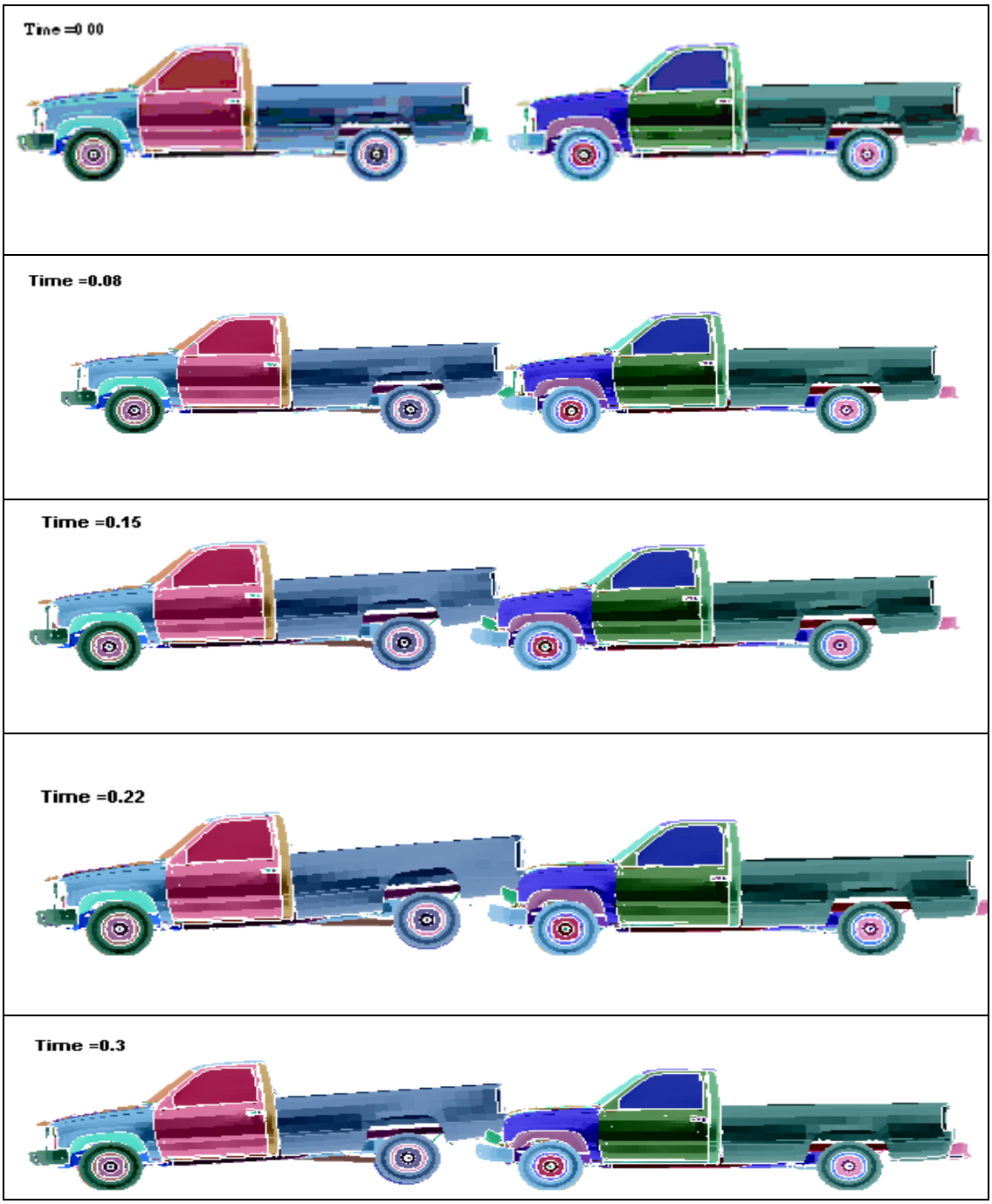

Figure 6.6. Simulation at low speed of 15mph

Simulation of the Chevy truck impacting the target vehicle can be seen in Figure 6.6.

In this case a similar Chevy truck impacts the rear end of truck at low speeds of the vehicle. Here also, the bumper of the truck underrides and contact between the two bumpers takes place for less then 0.08 secs.

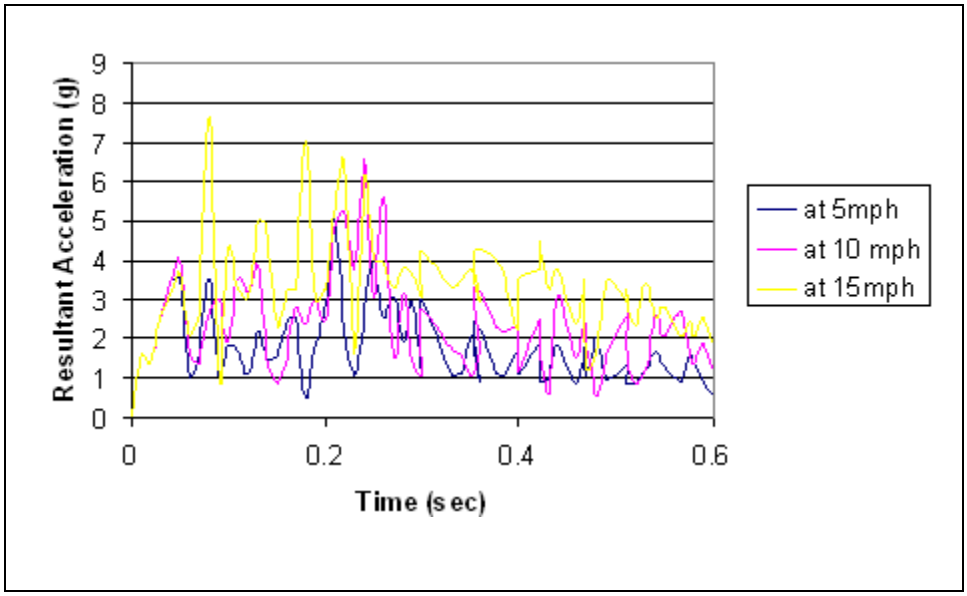

Figure 6.7. Resultant acceleration graphs from impact by Chevy truck.

There was an increase in acceleration level to be observed in figure 6.7 compared to case1. Maximum acceleration was 5 g at 5-mph and 6.2 g at 10-mph. highest acceleration was 7.8 g at 15-mph. For simulation of 0.6 secs, it was observed that acceleration pulses try to settle down slowly after 0.5 secs.

6.6 Case (3) Impact speed of Ford Taurus at 5,10&15 mph

Rear end kinematics for Ford Taurus (bullet vehicle) and Chevy truck (target vehicle) are shown in Figure 6.8 in different time frames. There was overlap between the bumper beams of the two vehicles at the point of engagement.

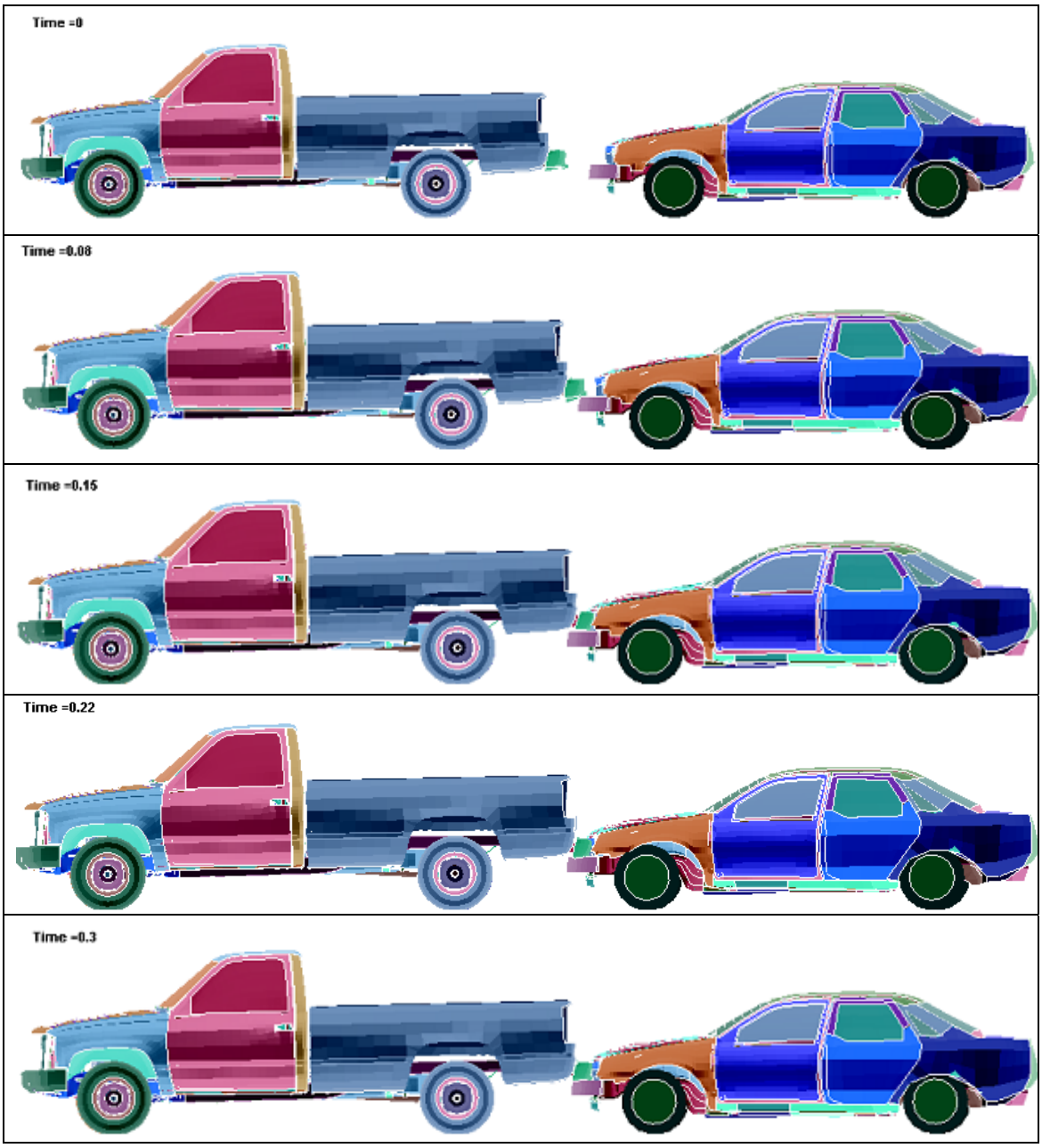

Figure 6.8. Simulation at low speed of 5mph.

Impact simulation of the Ford Taurus impacting the Chevy truck at 5 mph is shown in Figure 6.8. Acceleration level recorded at the load cell for different speeds is shown in the figure 6.9

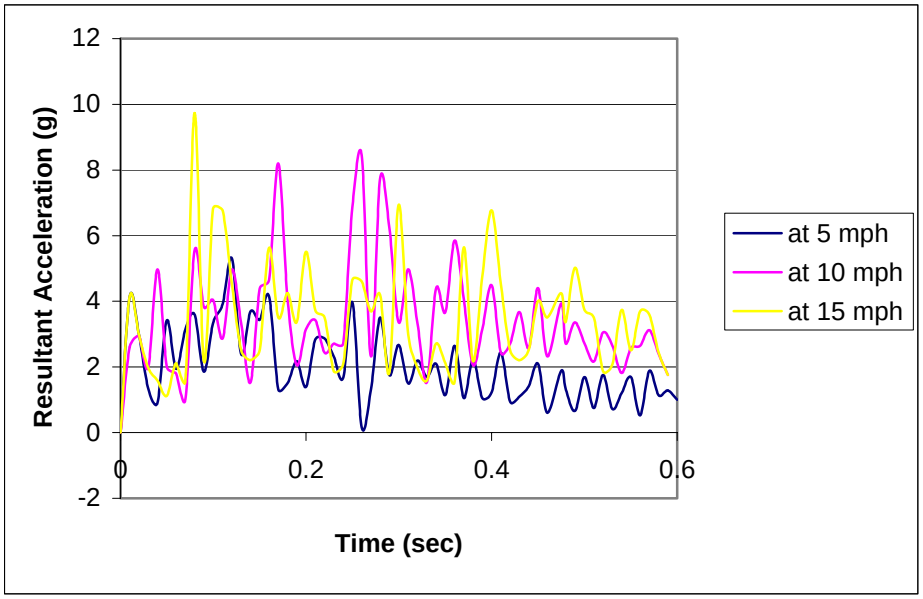

Figure 6.9. Resultant acceleration graphs from impact by Ford Taurus.

Maximum g's was 5.2 at 5-mph and 8.1 at 10-mph. There was variation in acceleration for 10-mph and 15-mph. Acceleration increases much earlier in case of impact at 15-mph and decreases very rapidly. At 10-mph the acceleration reaches higher to 8 g's much closer to 0.2 secs. The Acceleration levels of 10 g's is observed in Figure 6.9, due to vehicle weight and increase in velocity shows that acceleration increases during initial time period of 0.1 secs and then it decreases below 2 g's at 0.25 secs.

6.7 Case (7) Impact speed of Ford single unit truck at 5, 10,15 & 20 mph

Ford single unit truck impacts the low weight target vehicle at low speed. Simulation sequence for 0.3 secs is shown in Figure 6.10.From the bumper geometry, the bumper beams of the Ford heavy truck were above that of Chevy truck.

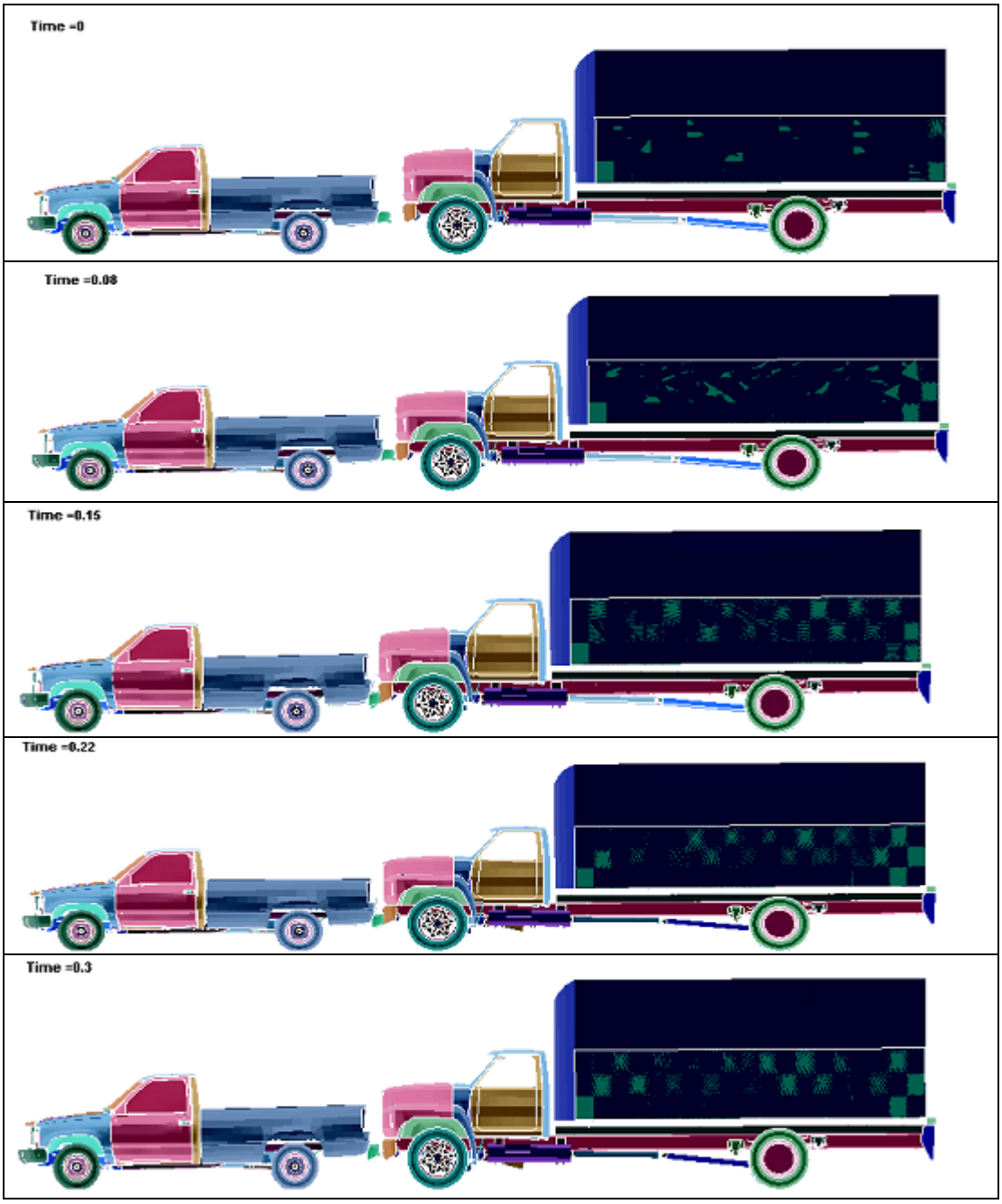

Figure 6.10. Simulation at low speed of 5 mph.

Bumper of bullet vehicle engages with rear bumper of the truck to cause override. It results in damage to the rear of the truck as the speed increases from 5 mph to 15 mph.

Simulation effect of the heavy large truck on Chevy truck at 5 mph is shown in Figure 6.10.Similar to all the other simulation, the acceleration increased at the point of impact before 0.08 secs. Target vehicle, Ford large single unit truck impacts the vehicle at 5, 10, 15 &20 mph.

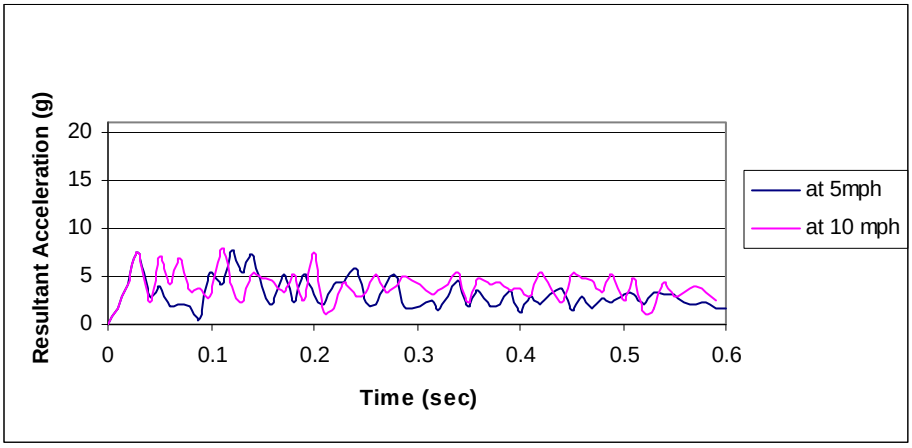

Figure 6.11. Resultant acceleration graphs from impact by Ford heavy truck.

Acceleration was compared for 5 mph and 10 mph as shown in Figure 6.11.Peak level of acceleration was 7 g and 8.2 g. These levels were very low in relation to graphs shown in Figure 6.12.

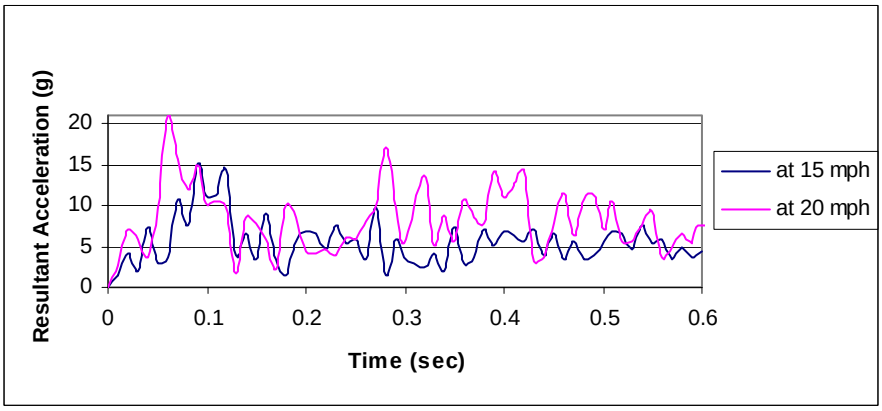

Figure 6.12. Resultant acceleration graphs from impact by Ford heavy truck.

In this case the impact speed was increased to 20 mph to study its occupant response for higher weight. The acceleration level was observed to 7 g at 5mph, 8.2 g at 10 mph and 15 g at 15 mph. Maximum acceleration was reached at 20 g for 20 mph. There was 3 times increase in acceleration for increase in speed from 5 mph to 20 mph. Bumper of the bullet vehicle engages very quickly with the target vehicle at 20 mph. After the disengagement of the bumpers, the bumpers get deformed and the acceleration level decreases with time.

It was observed from all the cases that the acceleration pulses of the accelerometer are sensitive to small contact. Graphs of these pulses at an increasing speed of 5 mph to 20 mph gives the comparative analysis of the momentum, mass and velocity of the vehicle. Momentum of the vehicle depends on the mass and velocity of the vehicle. In this study, momentum was transferred from bullet vehicle to the target vehicle. Different weights of the body had significant effect on the target vehicle.

6.8 Comparison of Results

Graph shown in Table 6.5 compares acceleration (g) for all cases of impact. The numbers of bullet vehicles are arranged according to weight of the vehicle and the speed with which it impacts the target vehicle.

Table 6.5. Comparison of acceleration for all cases of impact.

Bullet Vehicles →	**Geo Metro**	**Chevy Pickup Truck**	**Ford Taurus**	**Large ford Truck**
Weight →	*865 kg*	*1236 kg*	*1594*	*8000 kg*
↓ *Impact Speed*	Peak acceleration in truck (g)			
5 mph	4.5	5.0	5.2	7.5
10 mph	5.5	6.5	9.1	8.2
15 mph	6.0	7.5	9.8	15.0

The maximum acceleration level is 21 g in case of the heavy truck impacting at 20 mph as show in table 6.5.The weight of 8000 kg of heavy truck had sudden increase in peak acceleration from 8.2 g at 10 mph to 15 g at 15 mph. In this study the shape of the bumper is neglected to take into consideration is effect on bumper parts. Table 6.5 shows that acceleration increases with the increase in the speed. Also at 20 mph, simulation gave the maximum acceleration of 21 g. Due to mass and stiffness of the vehicle actual acceleration pulses can vary, while considering all the factors of the FE models.

CHAPTER 7

DYNAMIC SIMULATION OF OCCUPANT RESPONSE

7.1 Dummy and Seat Model

The code ECM is a pre and post processor used for modeling the 3D model and analyzing the results. In case of the low speed rear impact, the acceleration obtained at the center of gravity of the car seat, from Dyna analysis was used as a pulse for the acceleration of the the dummy in madymo. The response of the dummy was used for injury analysis.

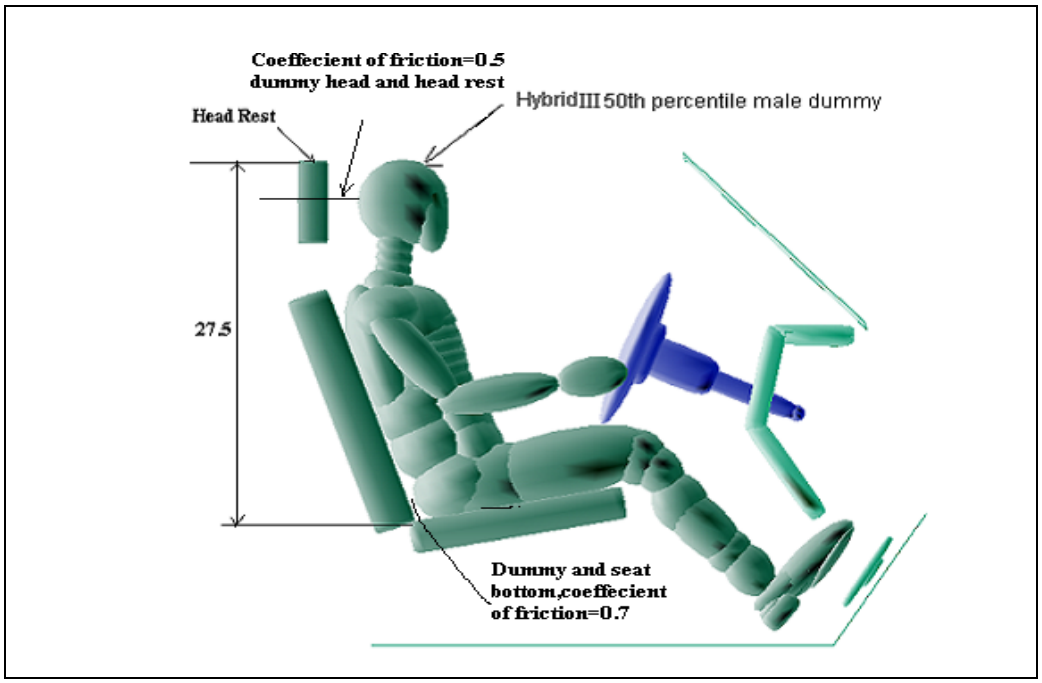

Figure 7.1. Dummy positioned on ellipsoidal seats.

The position of the dummy was arranged with the standard seating position of the occupant. Dummy model was merged with seat model with proper position as shown in Figure 7.1. The center of the head restraint is positioned along the axis of center of gravity of the head of the dummy. Body properties were given to the seat. The required dummy was selected and merged with the seat. Friction coefficient between the dummy and seat bottom was defined in the between the dummy and ellipsoidal seats, acceleration pulse, which is in terms of g's, is given to dummy as a whole body. These parameters were given to the input file of the MADYMO. The xml file of the whole system is run in MADYMO.The output file is opened in the Hyperview to get the required injury criteria.

The interior of the car consists of dummy and seat. The seat belt was ignored, as in this case its low speed and belt doesn't have significant effect on the dummy. The dummy translates rearwards in case of rear impact and the belts were used to prevent the dummy in forward motion. In Madymo model the car seat remains fixed and had contact relation with the dummy.

The two different criteria are studied in this case

1) Seat model with headrest
2) Seat model without headrest.

The possible injury for rear impact due to this study was compared with standard injury parameters. The effects of 26 simulations in Madymo were studied and compared for the different acceleration pulse on the dummy.

7.2 Effects on Dummy Response with Head Restraint

Simulation begins with relative velocity at 5mph from Rear end impact by Geo Metro. Sequence of dummy response from the acceleration pulse at 5 mph is as shown in Figure 7.2.

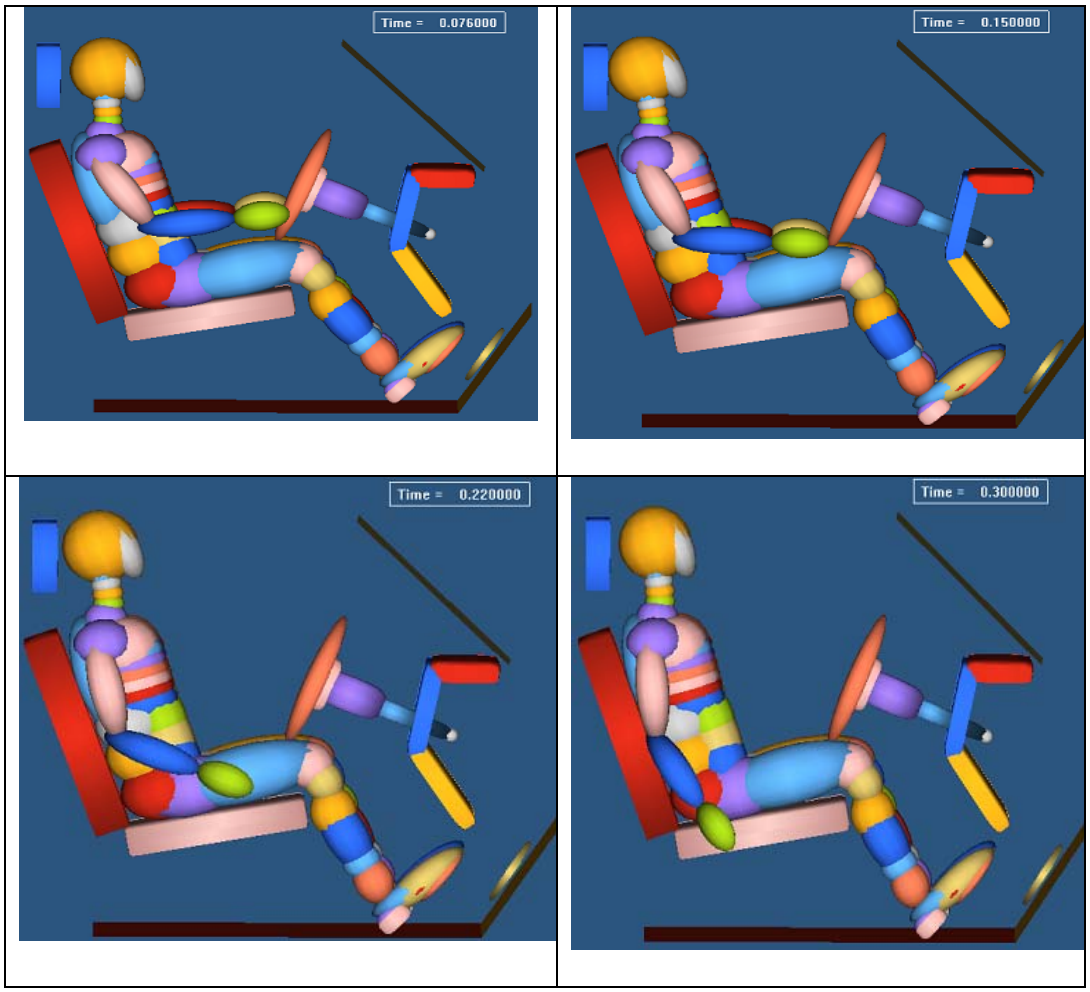

Figure 7.2. Simulation of dummy at relative velocity of 5mph.

The simulation sequence of Truck seat model with occupant in it is represented in Figure 7.2. The acceleration pulse loaded to the system is extracted from impact of Geo metro with Chevy truck with relative velocity of 5mph.Initial position of the

dummy is shown in Figure 7.1. At Position 1 at 0.076 ms; femur of the dummy gets lifted. Next position at 0.15 secs shows that the head touches the head restraint and the femur touches the steering wheel. The last two positions show that dummy are pushed forward by seatback and head lags by small amount due its inertia. The neck injury criteria N_{ij} is calculated and four distinct injury criteria, namely tension-extension (N_{te}), tension flexion (N_{tf}), compression-extension (N_{ce}) and compression-flexion (N_{cf}) are compared for all the cases of the rear impact. The injury criteria for the simulation at relative velocity of 5,10 and 15 mph were compared.

7.2.1 Comparisons of injury value for Geo Metro

Injury values of the neck injury predictor N_{ij} were obtained from the analysis file. These values were compared for speeds at 5,10 and 15 mph.

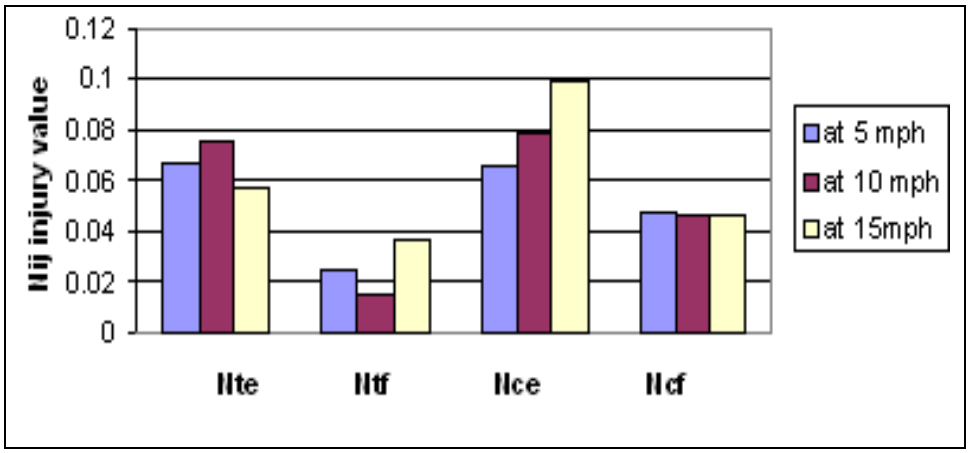

Figure 7.3. Comparison of injury value for dummy by Geo Metro.

The graph of rear impact by Geo Metro shown in Figure 7.3 indicates that injury value reaches maximum value of 0.1 in case of 15 mph impact. The values of neck compression extension are more for all the case. It shows that neck bends higher with compression extension moment and neck moves forward with smaller tension flexion.

7.2.2 Comparisons of injury value for Chevy truck

Acceleration pulse had impact on dummy and with head restraint postion; the injury values from the madymo were compared in Figure 7.4.

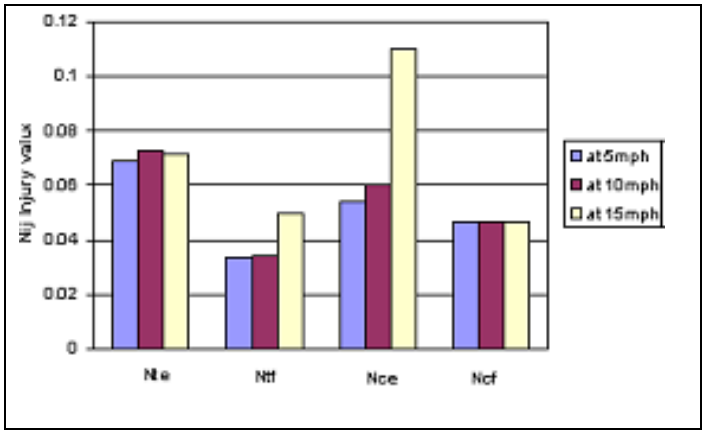

Figure 7.4. Comparison of Injury value for dummy by Chevy truck.

Figure 7.4 shows that compression extension (N_{ce}) is highest to the value of 0.15 at 15 mph. The neck compression flexion was low and same for all speeds. The Tension extension was also lower than 0.1.Effect of acceleration pulse can be seen on dummy, in which dummy moves back is show in Figure 7.5. The kinematics can be generally described as follows:

1) The head and torso translated backward together from their initial position.
2) The center of head restraint contacted the occiput of the head, thereby limiting backward rotation of the head.
3) The head was pushed forward while torso rebounded.

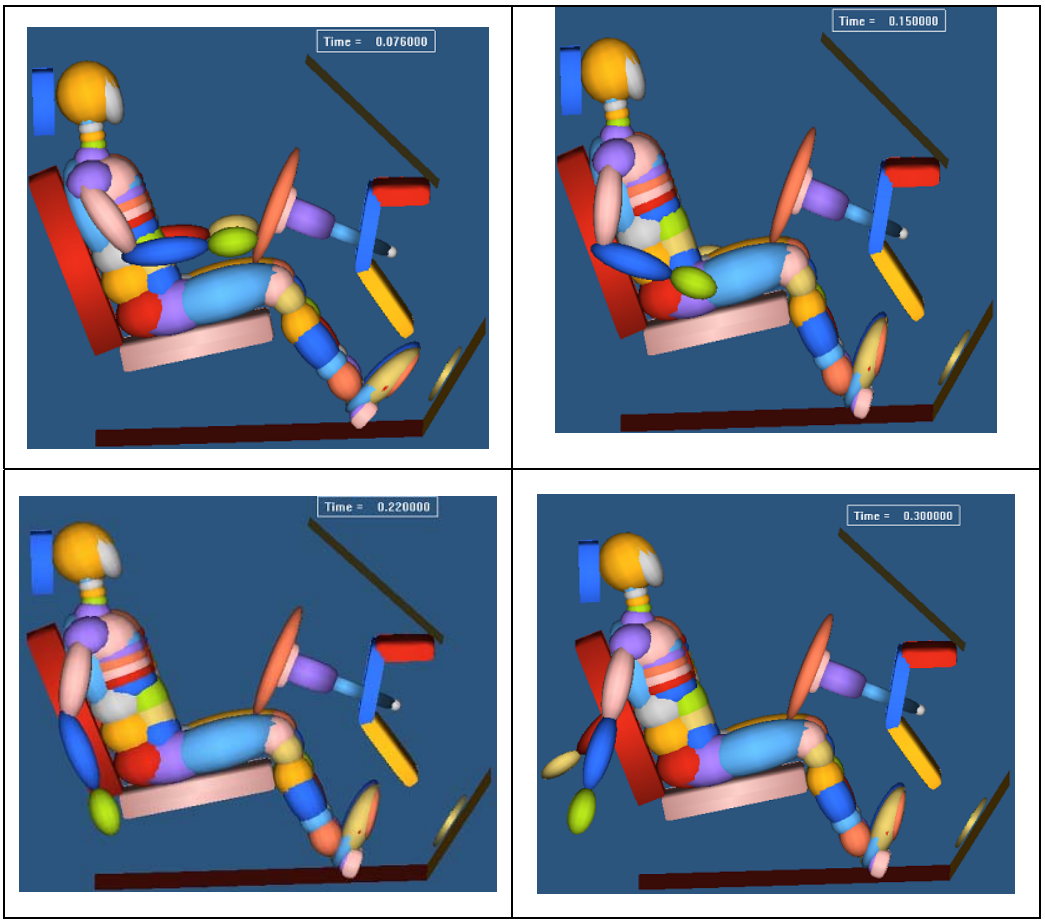

Figure 7.5. Simulation of dummy at relative speed of 15 mph.

There was a small amount of head rotation; this was due to stiffness of the neck in hybrid III dummy. The head translates rearwards with respect to cervical spine. Due to low translation, the injury values that were found out were very low and it does not have much effect on the neck response.

7.2.3 Comparisons of injury value for Ford Taurus

Injury values of the Hybrid III dummy model were obtained and compared for all speeds of impact.

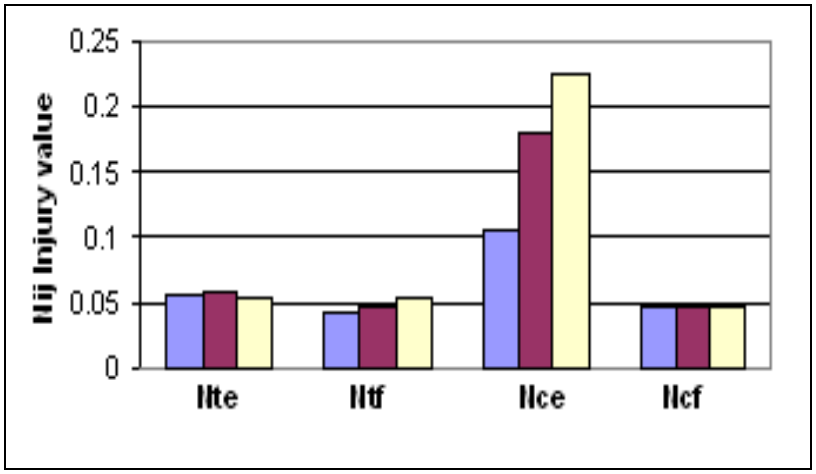

Figure 7.6. Comparison of Injury value for dummy by Ford Taurus.

The N_{ce} is at the value of 0.225 at 15 mph for impact by ford Taurus as shown in Figure 7.6. Neck tension extension, neck tension flexion and neck compression flexion are relatively same and very low. It doesn't have much effect in flexion. The head rotation in rearward is comparatively little more then in case of Geo metro from Figure 7.3. The rate of compression extension values shows that head restraint prevents the backwards rotation of dummy head in anticlockwise direction. Due to this the neck gets compressed. But the injury values were compared to the threshold values of neck injury predictor N_{ij} .It was observed that N_{ij} values were low and did not have relative effect on the head and neck of dummy.

7.2.4 Comparisons of injury value for large Ford heavy truck

Simulation of acceleration pulse effect on dummy by heavy truck shows the injury values. These values are compared and shown in Figure 7.7.

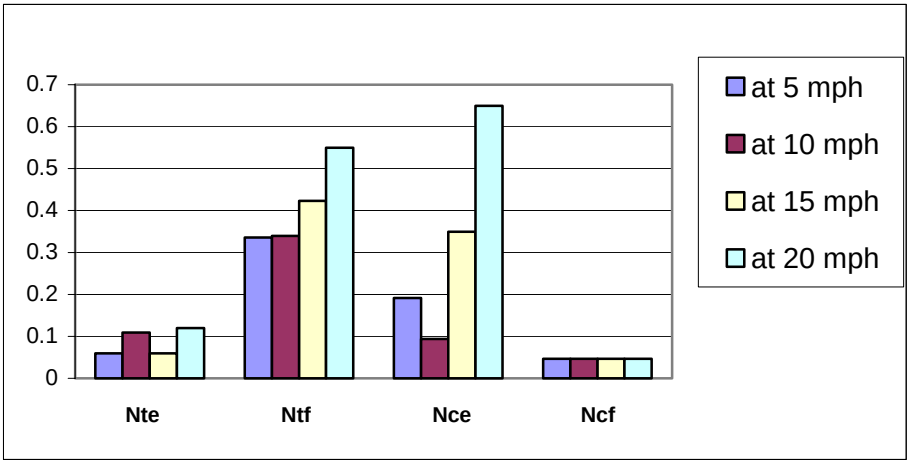

Figure 7.7. Comparison of Injury value for dummy by Ford heavy truck.

In the graph as shown in Figure 7.7, there is an additional simulation of the rear impact response at 20 mph. The values of N_{te} at 0.1 are lower; similarly for N_{cf} at 0.005, injury value remains same for all the conditions of different weights of the car. N_{tf} level is more at 20 mph and its level is same at 5 and 10 mph. Nce was very higher for the impact at 20 mph compared to the values at 5, 10 and 15 mph. Although these values are low there is no significant effect on the cervical spine. Head rotates more backwards with the neck N_{ce} reaching value of 0.64.Unsually; N_{ce} was less at 10 mph, less than the value at 5 mph.

7.3 Effect of Seat Model With No Head Restraint on Dummy

Headrest on the seat model was removed and the effect of acceleration pulse was observed for various low speed impacts. Simulation in Figure 7.8 shows response of the dummy for target vehicle impacted by Geo metro

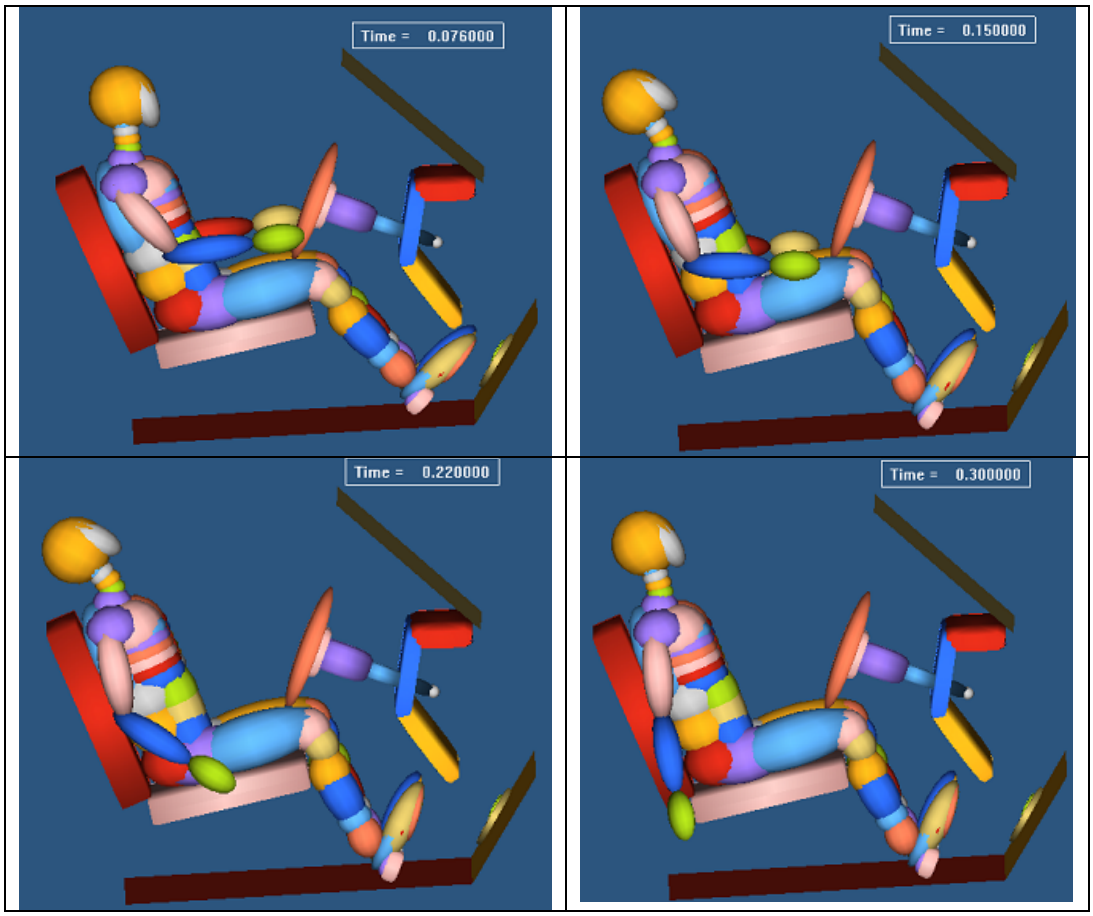

Figure 7.8. Simulation of dummy at relative velocity of 5mph.

The head kinematics of the dummy is shown in Figure 7.8. The dummy without Geo Metro impacts head restraint with acceleration pulse of 15 mph it shows that

1) The head and torso translates backward together from initial position,
2) The head rotation was more as there is no head restraint,
3) Due to stiffness of the neck the head returns to the original position with the flexion in the neck.

7.3.1 Comparisons of injury value for Geo Metro

Injury values of the neck injury predictor N_{ij} were obtained from the analysis file. These values were compared for speeds at 5, 10 and 15 mph.

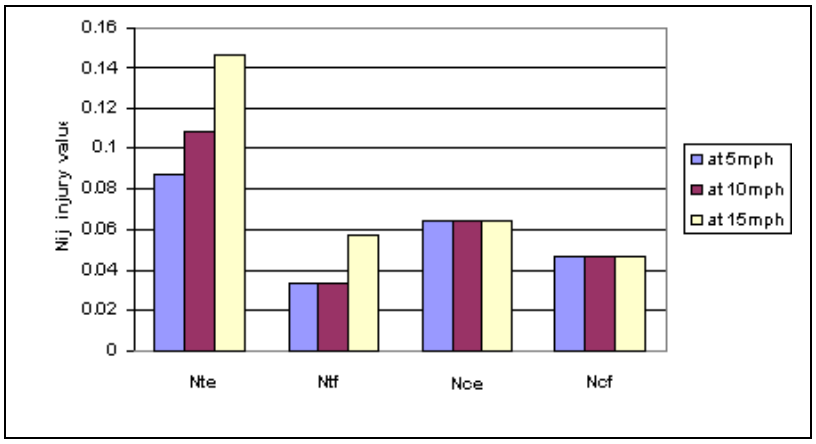

Figure 7.9. Comparison of Injury value for dummy by Geo Metro.

As seen in Figure 7.9 N_{te} is more compared to N_{ce}. The neck compression flexion was same for all speed and it doesn't have significant effect on the neck in both the cases of the head restraint. Compression extension was lower, due to the lack of head restraint, as there is no rigid body constraining the head that causes compression. N_{te} increases with the increase in speed of the vehicle. Overall neck tension extension values are low and injuries due to increase in speed are not taken into affect, as it's very low to see the possible neck injuries in occupant.

7.3.2 Comparisons of injury value for Chevy truck

Dummy response from the pulse by Chevy truck gives the injury values. These injury values are compared in Figure 7.10.

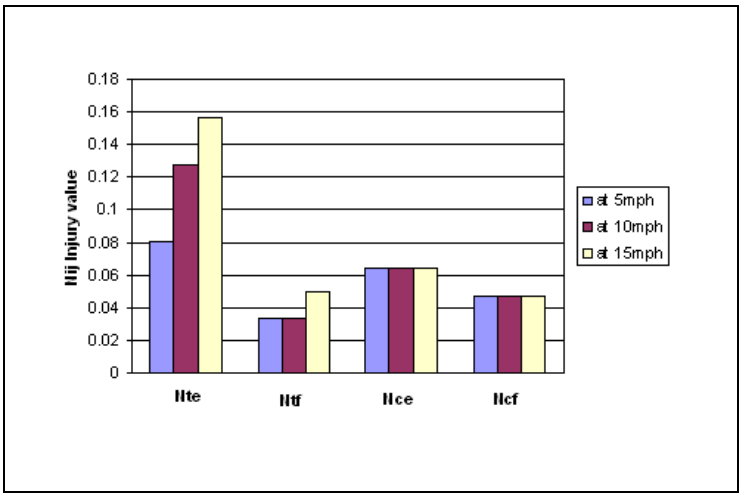

Figure 7.10. Comparison of Injury value for dummy by Chevy Truck.

The neck tension extension reaches the values of 0.15 while the neck tension flexion, neck compression extension and neck compression flexion are very low. N_{cf} is 0.46 and it remains stable for all the impact, also for N_{tf} values are less then 0.05, which are very low, can be neglected to take into consideration of the impact injury .N_{ce} values are seen stable and varies with the weight.

7.3.3 Comparisons of injury value for Ford Taurus

Similarly in the this case of rear impact by ford Taurus as seen in Figure 7.11 the neck tension extension was more, which reaches the value of 0.2.The values of neck tension flexion, neck compression extension and neck compression flexion remains lower than 0.1.These comparisons shows that no suitable injury is observed as it does not reaches the critical injury value of N_{ij} of 1.

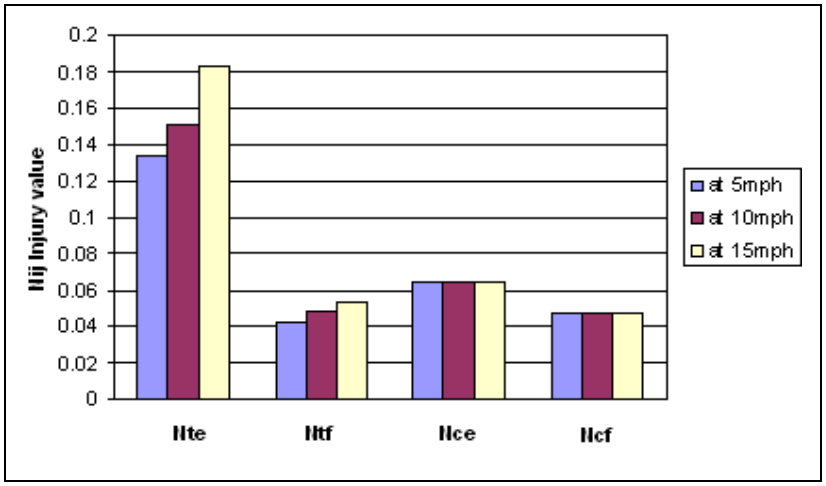

Figure 7.11 Comparison of Injury value for dummy by Ford Taurus

The values of N_{te} are 0.13, 0.15 and 0.18 for speed at 5-mph. Forces acting on the neck and the related moments were low and the injuries were considered negligible. In the next case of simulation, the relative speed of the heavy truck vehicle was increased to 20 mph. This was done to understand the effect of the weight and increase in speed on the hybrid III dummy model.

The simulation of the effect of dummy without head restraint, when the Ford single unit truck was impacted at 15 mph without the head restraint is shown in Figure 7.12.Dummy response for 0.3 secs showed that without head restraint, the motion of head was rotated in anticlockwise direction and had effect on the neck due to higher moments in rotation.

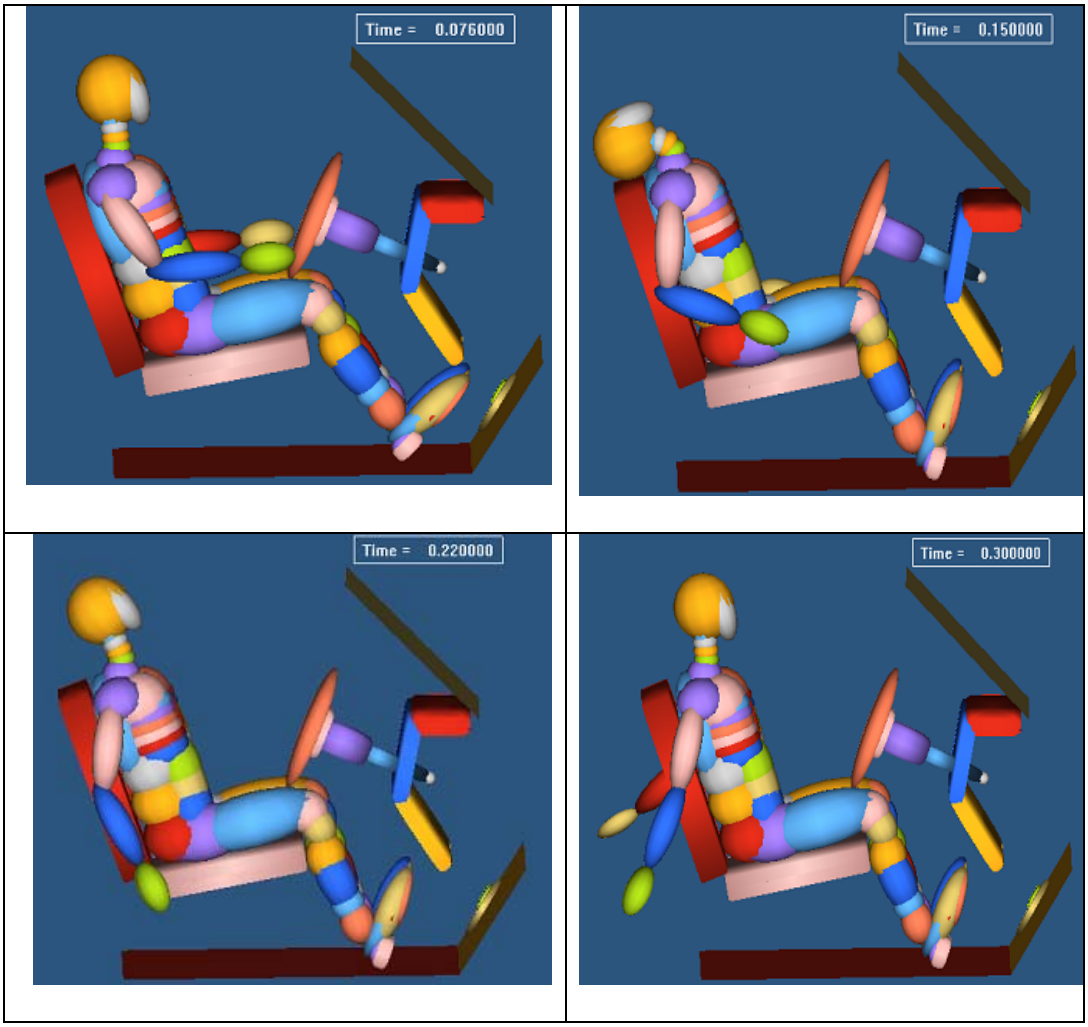

Figure 7.12. Simulation of dummy at relative velocity of 5 mph.

7.3.4 Comparisons of injury value for large Ford heavy truck

The Figure7.12 shows the animation sequence in which the head moves completely back with extension of the neck at 0.15 secs and the neck returns to same place at the end of 0.3 secs

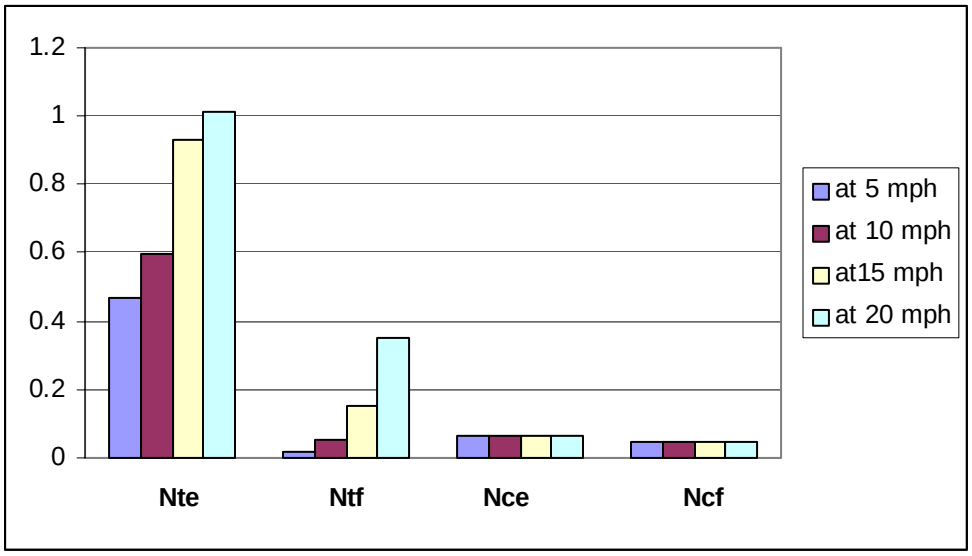

Figure 7.13. Comparison of Injury value for dummy by Ford heavy truck.

The acceleration from the heavy truck impact is very high and there is sudden increase in value of neck tension extension. It reaches a value of more then 0.8 with amount of 15 g's the injury is probably less than 1 which is critical injury value for the hybrid III dummy.

To observe the effects of the speed on the dummy, the truck speed was increased to 20 mph. From the graph, clearly there was increase in value of N_{te} at 1.1. This injury values reaches more then the critical limit of standard Hybrid III dummy model and potential injury was observed. The injury effects were unknown, but the probability of the injury at such speed can occur was known and effect of the weight and relative speed of the finite element model impacting the vehicles on the occupant is studied.

CHAPTER 8

COMPARISONS AND DISCUSSIONS

8.1 Comparisons of Acceleration Pulses

Maximum acceleration was measured at the center of gravity of the seat of the Chevy truck. There were four three different parameters which affects the acceleration, the speed of the bullet vehicle, weight of the vehicle and the full impact. Variation in speeds and weight had effects on g's of acceleration.

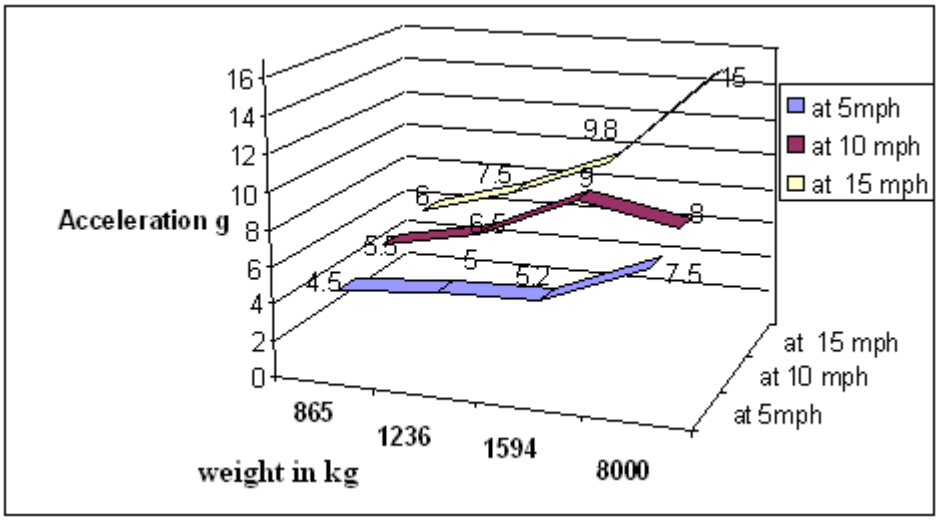

Figure 8.1. Acceleration in truck in g as a bullet vehicle impacted at different mass and speed by target vehicle.

It is clear from the Figure 8.1 that weight of 8000 kg large truck has effect on acceleration levels. The momentum of vehicle is due its mass and velocity. So with increase in mass, there is increase in velocity. Bacic principle of momentum is conserved; the momentum is transferred from bullet vehicle to the target vehicle. Maximum of 15 g was observed at 15 mph. Vehicle velocity of the heavy truck was further increase to 20 mph.

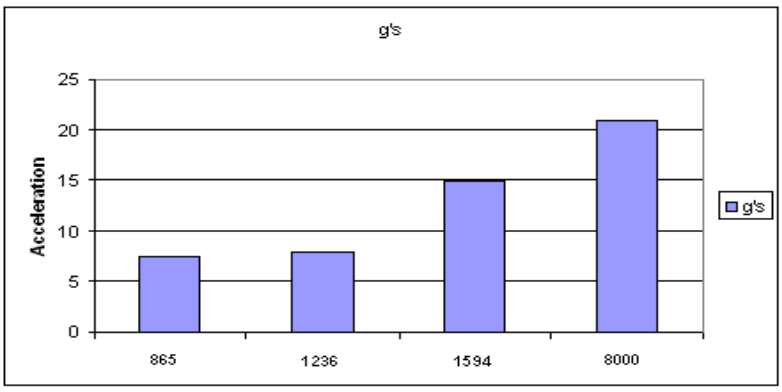

Figure 8.2. Comparison of g at 20 mph.

The Figure 8.2 shows that the heavy truck of the weight 8000 kg was further impacted at 20 mph to the rear end of the target vehicle. Amount of g was increased from 7.5 at 5 mph to 21g at 20 mph. Acceleration had increased to 3 times more, from the speed at 5 mph to 20 mph. Maximum g's from the center of the gravity of seat was used to study its effect on occupant motion in MADYMO.

8.2 Neck Injury Values

The Table 8.1 and 8.2 shows main injury values of $N_{ij.}$

Table 8.1 Dummy responses for seat with head restraint

	Speed	N_{te}	N_{tf}	N_{ce}	N_{cf}
Small size car	at 5 mph	0.06	0.02	0.06	0.04
	at 10 mph	0.07	0.01	0.07	0.04
	at 15 mph	0.05	0.03	0.09	0.04
Chevy truck	at 5 mph	0.06	0.03	0.05	0.04
	at 10 mph	0.07	0.03	0.06	0.04
	at 15 mph	0.07	0.04	0.10	0.04
Medium size car	at 5 mph	0.05	0.04	0.10	0.04
	at 10 mph	0.05	0.04	0.18	0.04
	at 15 mph	0.05	0.05	0.22	0.04
Large size car	at 5 mph	0.05	0.03	0.19	0.04
	at 10 mph	0.10	0.03	0.09	0.04
	at 15 mph	0.05	0.05	0.33	0.04
	at 20 mph	0.12	0.05	0.25	0.04

Table 8.1 Dummy responses for seat with no head restraint

	N_{ij}	N_{te}	N_{tf}	N_{ce}	N_{cf}
Small size car	at 5 mph	0.08	0.03	0.06	0.04
	at 10 mph	0.10	0.03	0.06	0.04
	at 15 mph	0.14	0.05	0.06	0.04
Chevy truck	at 5 mph	0.08	0.03	0.06	0.04
	at 10 mph	0.12	0.03	0.06	0.04
	at 15 mph	0.15	0.04	0.06	0.04
Medium size car	at 5 mph	0.13	0.04	0.06	0.04
	at 10 mph	0.15	0.04	0.06	0.04
	at 15 mph	0.18	0.05	0.06	0.04
Large size car	at 5 mph	0.47	0.02	0.06	0.04
	at 10 mph	0.60	0.05	0.06	0.04
	at 15 mph	0.93	0.15	0.06	0.04
	at 20 mph	1.01	0.35	0.06	0.04

Neck injury predictor values for all the impact simulation in MADYMO, which affected the motion of the head, were taken in consideration. Comparisons of bar graph for speeds at 5 mph and 10 mph at an increasing weight of 865, 1236, 1594 and 8000 kg for neck tension extension are shown in Figure 8.3.

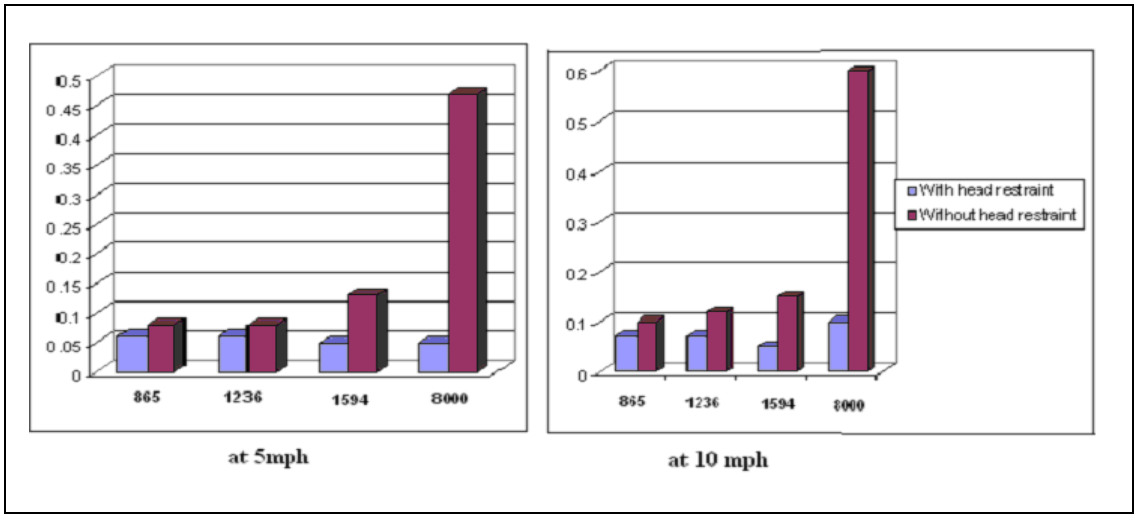

Figure 8.3. Neck extensions at 5 mph and 10 mph.

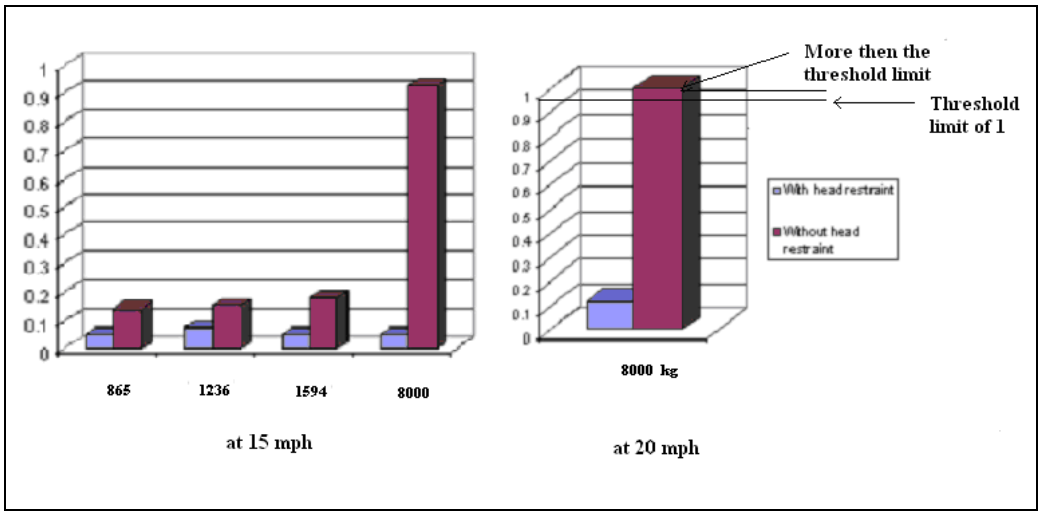

Figure 8.4. Neck extensions at 15 mph and 20 mph.

Figure 8.4 shows the comparison of neck tension extension with head restraint and without head restraint for neck extension at 15 mph and 20 mph. The rotation of the head is more at 5 mph with impact from heavy truck weight of 8000 kg. The relative motion between the head and the spine is more with the tension extension reaching value of 0.9.Weight and height of the heavy ford truck had affected the relative motion of head and neck. Value was less then critical parameter of 1 for hybrid III dummy. Simulation at 20 mph gave injury value more then the critical limit of 1 for Hybrid III dummy model. Moments in the head rotation had reached a limit and possible injury can be predicted. Due to increase in more then injury limit there is an estimate of 30 percent risk of AIS 2 neck injury, a 22 percent risk of AIS 3 injury, a 18 percent risk of AIS 4 injury and a 7 percent risk of an AIS 5 injury.

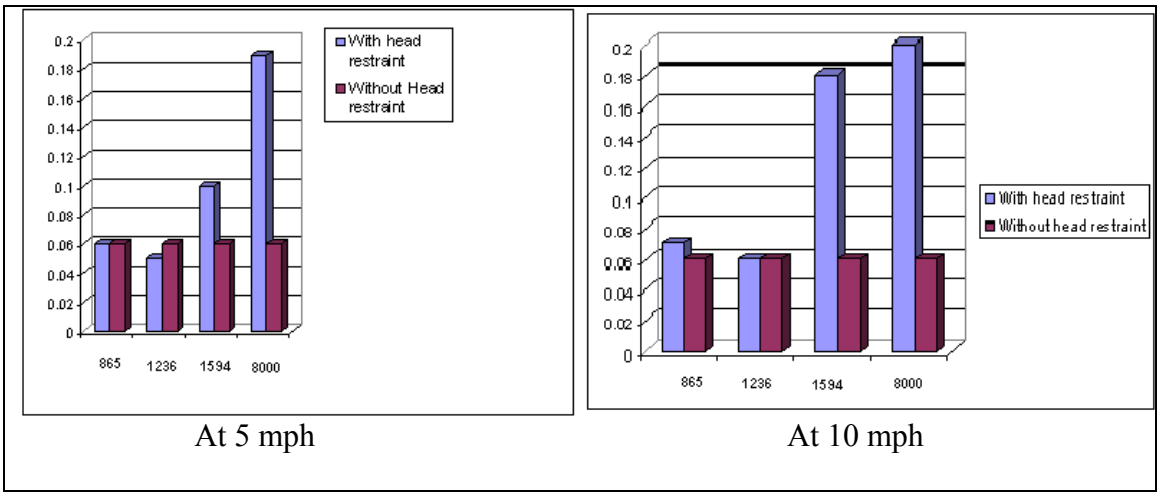

Figure 8.5. Neck extensions at 5 mph and 10 mph.

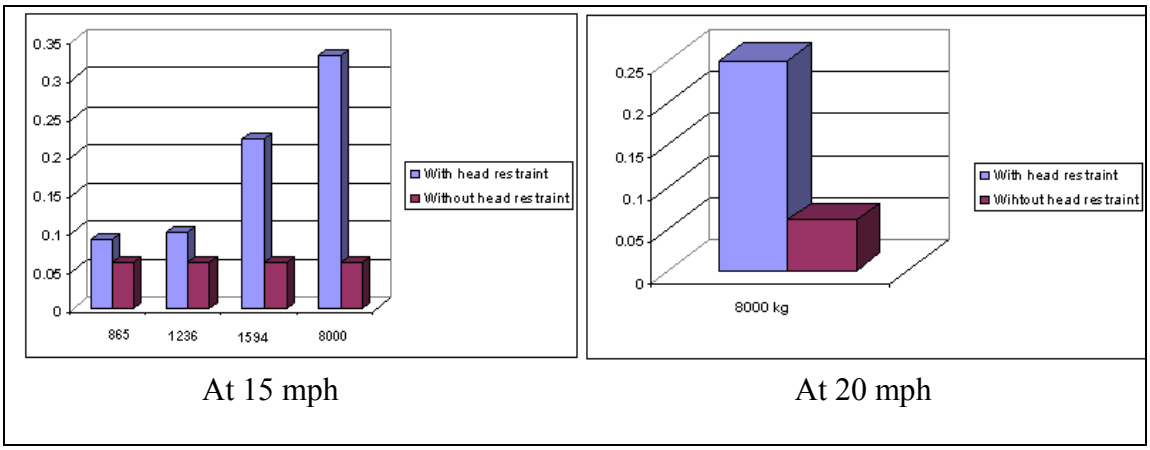

Figure 8.6. Neck extensions at 15 mph and 20 mph.

Here we can see from Figure 8.5 and Figure 8.6 that the neck compression is more in head restraint and less in without head restraint. The head rotation is restricted to move backwards producing compressive forces on the neck. Without head restraint this value is very less. The injury level is low at 5 mph and it increases at 15 mph to 0.32 and at 20 mph for weight of 8000 kg injury vale reaches to 0.25, but injury level is below the critical value.

CHAPTER 9

CONCLUSION AND RECOMMENDATION

9.1 Conclusions

FMVSS conducts the rear impact test at high speeds for all vehicles, to check the fuel spillage and check its performance. As there is no standard bumper regulation for low speed impact test, finite element model of the target vehicle i.e. Chevy truck was validated by impacting the rear bumper of truck with rigid wall. Results of the bumper were studied and it was verified that the deflection of the bumper was reduced to zero. This signifies that bumper material after the impact did not reached the yield strength of the bumper.

The main aim was to study the effect of the different weights of the vehicle on the target and study its impact response on the occupant. Four different weights of the vehicle at 865, 1236, 1594 and 8000 kg respectively were used to impact the target vehicle at the low speed of 5, 10 and 15 mph respectively. Acceleration curve were obtained from the load cell of the seat of the target vehicle. These curves in terms of g's were compared for all low speed impact. Acceleration level increases to 49 percent at 5 mph for increase in weight from 865 kg to 8000 kg. At 10 mph there is an increase of 44 percent of the g, but the maximum acceleration in g was observed to increase to 154 percent for 15 mph.

Impact of the occupant response was studied for possible injuries to the occupant. Injury values of the dummy were compared with standard injury value of Hybrid III model. With head restraint injury values were very low and neck compression extension

were more in all the possible neck injuries but were below the critical values of N_{ij} for the given dummy model used in the study. Similarly for dummy with no head restraint, neck tension extension was observed to reach 0.9 at 15 mph for heavy truck. To predict the potential injury, simulation of the heavy truck at 20 mph impacting the target vehicle was conducted. The N_{ij} value for neck tension extension increased to 1.01, which was greater than critical value of 1.0.With this N_{ij}, AIS value of 4 is expected which means at 20 mph, there is 30 percent chance of concussion or skull fracture, 22 percent chance of more than 15-minute unconsciousness without severe neurological damages, 18 percent chances of impresses skull fracture with severe neurological injuries, and 7 percent chance of more than 12 hours of unconsciousness with the hemorrhage in skull.

9.2 Recommendations

The following recommendations can be made on the study of low speed rear impact on truck:

- Dummy model can be coupled with the Chevy truck model to study the similar effects of neck injury on the occupants.
- Hybrid III dummy model can be replaced with the Bio-RID II model, to study the neck injury with better results.
- Madymo can be used to build test vehicles with rigid surfaces and ellipsoids, as the analysis time for the Dyna file is more than the Madymo.
- Study can be done by adding more features in rear of the Chevy truck to prevent the underride i.e. compatibility of truck with other vehicles.

REFERENCES

LIST OF REFERENCES

Avery M., Weekes, A. (July 2006). "The development of a new low speed impact test to improve bumper performance and compatibility," Thatcham, Berkshire, I Crash, Volume 8, Paper number 9, Page Numbers 1-12.

Butala, K., (May 2004). "Study of rear end vehicle to vehicle impact crash analysis," Masters Thesis, Wichita State University.

Bostron, O., (July 1999). "Comparisons of car seats in low peed rear-end impacts using BioRID dummy and Neck Injury Criterion," Accident Analysis and Prevention, Volume 32, Issue 2, Page Numbers 321-328.

Bois, P.D., Choubahig, C., Fileta, B., Khalil, B., Albert, I., Hikmat K .F, Harold M., Wismans, M., (May 2000). "Vehicle crashworthiness and occupants protection," Automotive Application Committee, Southfield, Michigan, SAE, Document Number 2000-05-8956.

Calso, S.M., Saha, N. K., Faruque, M.O., (1993). "Simulation of offset and in-line car to car rear impacts," Crashworthiness and Occupant Protection in Transportation Systems, ASME, Volume 169, Page Numbers 149-160.

Derosia, J., Yoganandan, N., Pintar, F A., (October 2003). "Rear impact response of different sized hybrid III dummies", Department of Neurosurgery, Milwaukee, Wisconsin, Neuroscience Report, Volume 21, Paper no 433, Page Numbers 50-55.

Forero, A. K., **(**Jan 2005). "Influence of seat optimization based on one dummy size on the risk of whiplash injury for different size occupants," Crash Safety Division, Chalmers university of Technology, Report Number 49, Page Numbers 25-47.

FHWA/NHTSA National CrashAnalysis Center, (1992). www.ncac.gwu.edu.

Heinrichs, B. E., Lawrence, J .M., Allin, B. D., Bowler, J. J., Wilkinson, Ising W. and King, D. J., (2001). "Low speed testing of pickup truck bumpers," Machine Engineering Associates, Society of Automotive engineers, Document No 2001-02-0893, Page Numbers 187-194

Insurance Institute for Highway Safety, (April 2002). "Frontal offset crashworthiness evaluation guidelines for rating injury measure," Volume 5, Page Numbers 1-5.

Insurance Institute for Highway Safety (IIHS), (2002),'Low-speed crash test protocol', Insurance Institute for Highway Safety (IIHS), Arlington, VA, Status Report, Volume Number 9, Page Numbers 6-17.

Kumbhar, S., (Dec 2006). "Development of finite element model and analysis of rear impact scenario of a low-floor mass transit bus," Masters Thesis, Wichita State University.

Kleinberger, M., Sun, E., Saunders, J. and Zhou, Z., (1999). "Effects of head restraint position on neck injury in rear impact-paper," Traffic Safety and Auto Engineering, Washington, D.C, SAE, Page Numbers 4-28.

Linder, A., Avery, M., (2003). "Change of velocity and pulse characteristics in rear impacts real world and vehicle tests data," Motor Insurance Research Center, Sweden, Paper Number 285, Page Number 5-15.

"LS DYNA keyword user manual," version 970, (April 2003). LSTC.

"MADYMO reference manual V6.1", (April 2001). TNO Automotive.

National Highway Traffic Safety and Administration, (2004). "Huge costs of bumper mismatch," Status Report, Volume 39, Paper Number 9, Page Numbers 5-20.

National Highway Traffic Safety Administration, (1977). "Title 49 Code of Federal Regulations Part 581, Bumper Standard," National Highway Traffic Safety Administration (NHTSA), Washington, DC, Volume 2, Page Numbers 23-35.

Ragland, C. L., (1997), "Research tests to develop improved FMVSS 301 rear impact test procedure," National Highway Traffic Safety and Administration, U.S, Paper No 98s4p16, Page Numbers 907-910.

Schmitt, K.U., Muser, M. H. and Niederer, P., (2001). "A new Neck Injury Criterion candidate for rear-end collisions taking into account shear forces and bending moments," Working group on accident mechanics, University and Swiss Federal Institute of Technology (ETH) Zurich, Switzerland, Paper No. 124, Page Numbers 1-9.

Shimamoto, N., Tanaka, M., "Developing experimental cervical dummy models for testing low speed rear-end collisions," Daihatsu motor company, Kyoto University, Japan, Paper No 98s9010, Page Numbers 1954-1961.

Svennson, M. Y., Bostrom, O., Davidson, J., Hanson, H., Haland, Y., Lovsund P., Suneson, A., Saljo, A., (2000). "Accident analysis and prevention Neck injuries in car collision a review covering possible injury mechanism and development of rear impact dummy of vehicle," Volume 32, Issue 2, Page Numbers 32-68.

Yuen, M. and Bilson, L .E., (2004). "Development of an antiwhiplash seat," Prince of Wales Research Institute, Australia, Australian Transport Safety Bureau, Paper number 21, Page Number 56-72.

Zellmer, H., Stamm, M., Seindenschwang, A., (2001). "Enhancement of seat performance in low speed rear impact," Autoliv GMbh, Department of Accident Research, Document Number 231, Page Number 1-10.

Zaouk, A K., Dr. Bedewi, N E., Dr. Kan, C D., and Marzougui, D., (1996). "Development and evaluation of a C-1500 pick-up truck model for roadside hardware impact simulation," NHTSA, National Crash Analysis Center, George Washington University, Volume 5, Page Number 1-14.